

# Perturbation Theory Reloaded

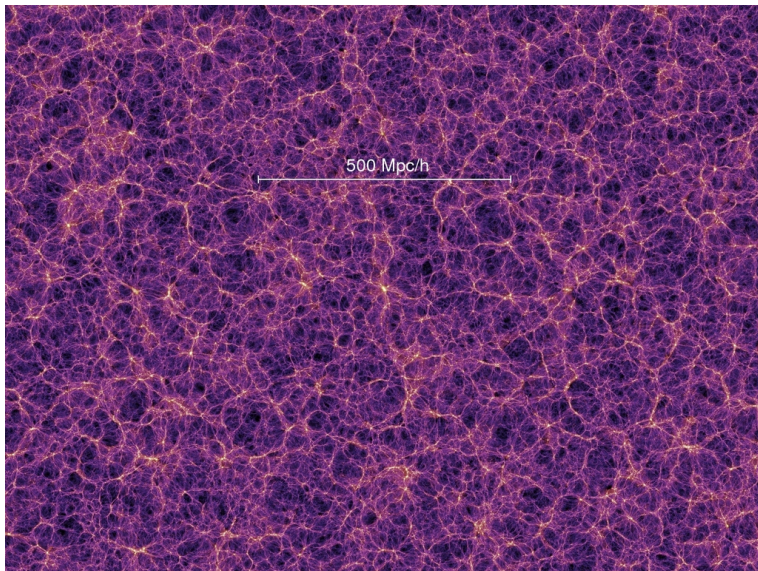
Modeling the Power Spectrum in High-redshift Galaxy Surveys

Eiichiro Komatsu

Department of Astronomy  
University of Texas at Austin

ITC Colloquium, May 15, 2007

# Large-scale Structure of the Universe (LSS)



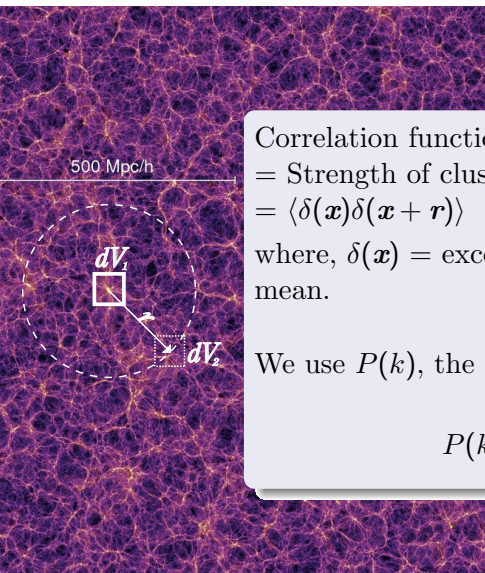
Millennium Simulation (Springel et al., 2005)

# LSS of the universe : What does it tell us?

- Matter density,  $\Omega_m$
- Baryon density,  $\Omega_b$
- Amplitude of fluctuations,  $\sigma_8$
- Angular diameter distance,  $d_A(z)$
- Expansion history,  $H(z)$
- Growth of structure,  $D(z)$
- Shape of the primordial power spectrum from inflation,  $n_s, \alpha, \dots$
- Massive neutrinos,  $m_\nu$
- Dark energy,  $w, dw/da, \dots$
- Primordial Non-Gaussianity,  $f_{NL}, \dots$
- Galaxy bias,  $b_1, b_2, \dots$

- ① One point statistics
  - Mass function,  $n(M)$
- ② Two point statistics
  - Power spectrum,  $P(k)$
- ③ Three point statistics
  - Bispectrum,  $B(k)$
- ④ Four point statistics
  - Trispectrum,  $T(k)$
- ⑤  $n$ -point functions

# The most popular quantity, $\xi(r)$ and $P(k)$



Correlation function  $\xi(r)$

= Strength of clustering at a given separation  $r$

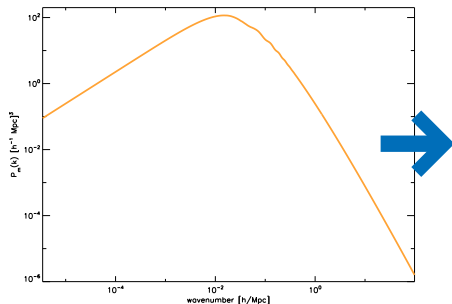
$$= \langle \delta(\mathbf{x})\delta(\mathbf{x} + \mathbf{r}) \rangle$$

where,  $\delta(\mathbf{x})$  = excess number of galaxies above the mean.

We use  $P(k)$ , the Fourier transform of  $\xi(r)$  :

$$P(k) = \int d^3\mathbf{r} \xi(r) e^{-i\mathbf{k}\cdot\mathbf{r}}$$

# How do we do this?



## Cosmological parameters

Matter density,  $\Omega_m$

Baryon density,  $\Omega_b$

Dark energy density,  $\Omega_\Lambda$

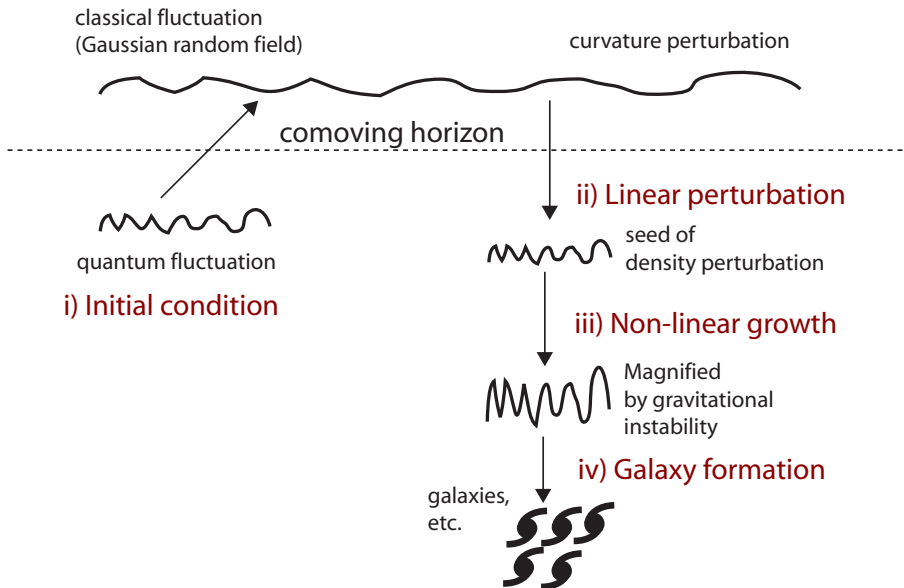
Dark energy eq. of state,  $w$

Hubble constant,  $H_0$

...

**We have to be able to *predict*  $P(k)$  very accurately, as a function of cosmological models.**

# Cosmological perturbation theory



# Initial Condition from inflation

- Inflation gives the initial power spectrum that is **nearly a power law**.

$$P(k, \eta_i) = A \left( \frac{k}{k_0} \right)^{n_s + \frac{1}{2} \alpha_s \ln \left( \frac{k}{k_0} \right)}$$

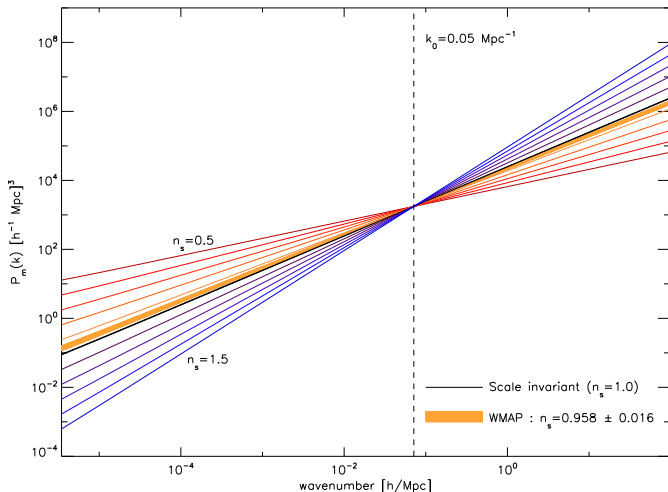
- Inflation predicts, and observations have confirmed, that

$$n_s \sim 1$$

$$\alpha_s \sim 0$$

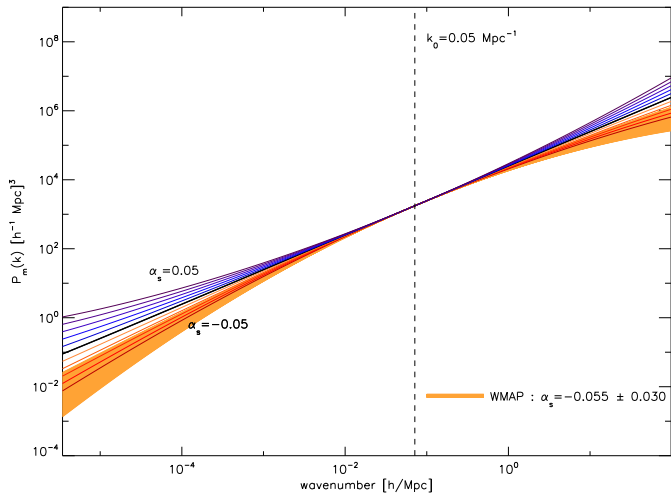
# Initial Power Spectrum: Tilting

- Initial matter power spectrum for various  $n_s$  :  $P(k) \propto (k/k_0)^{n_s}$



# Initial Power Spectrum: Running

- Initial matter power spectrum for various  $\alpha_s$



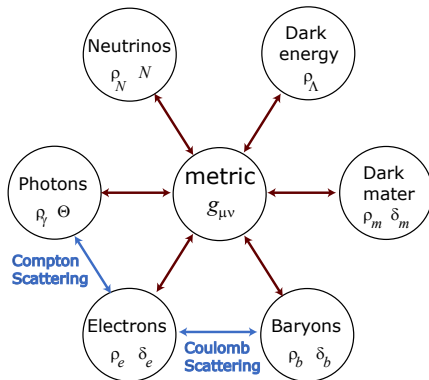
# Evolution of linear perturbations

- Two key equations
  - The Boltzmann equation

$$\frac{df}{d\lambda} = C[f]$$

- Perturbed Einstein's equations

$$\delta G_{\mu\nu} = 8\pi G \delta T_{\mu\nu}$$



# Basic equations for linear perturbations

- The equations for linear perturbations

- Dark matter

$$\delta' + ikv = -3\Phi' : \text{Continuity}$$

$$v' + \frac{a'}{a}v = -ik\Psi : \text{Euler}$$

- Baryons

$$\delta'_b + ikv_b = -3\Phi' : \text{Continuity}$$

$$v'_b + \frac{a'}{a}v_b = -ik\Psi + \frac{\tau'}{R}(v_b + 3i\Theta_1) : \text{Euler with interaction w/ photons}$$

- Photon temperature,  $\Theta = \Delta T/T$

$$\Theta' + ik\mu\Theta = -\Phi' - ik\mu\Psi - \tau'(\Theta_0 - \Theta + \mu v_b - \frac{1}{2}\mathcal{P}_2(\mu)\Theta_2)$$

- Gravity

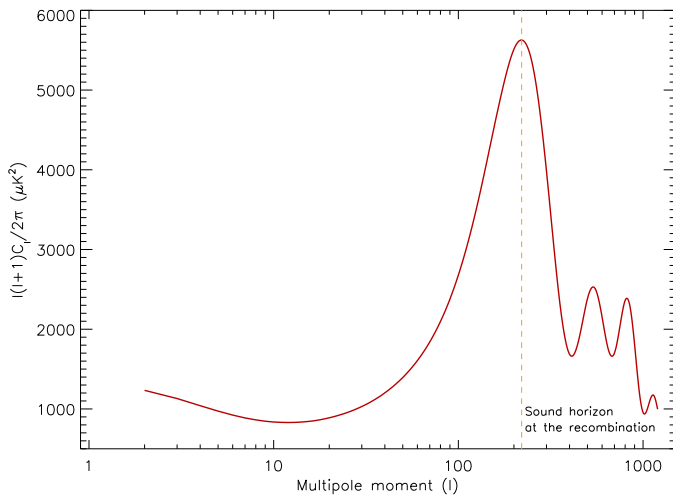
$$k^2\Phi + 3\frac{a'}{a}\left(\Phi' - \Psi\frac{a'}{a}\right) = 4\pi G a^2(\rho_m\delta_m + 4\rho_r\Theta_{r,0})$$

$$k^2(\Phi + \Psi) = -32\pi G a^2\rho_r\Theta_{r,2}$$

- These are well known equations.

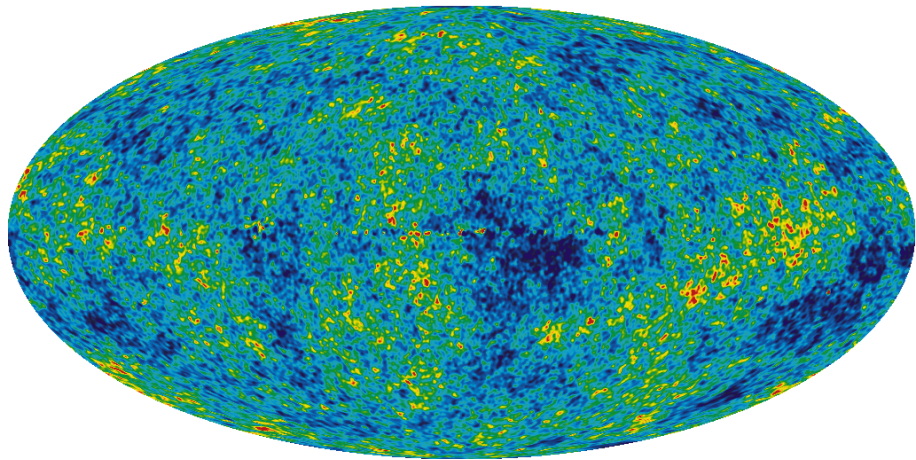
Observational test?

# Prediction: the CMB power spectrum



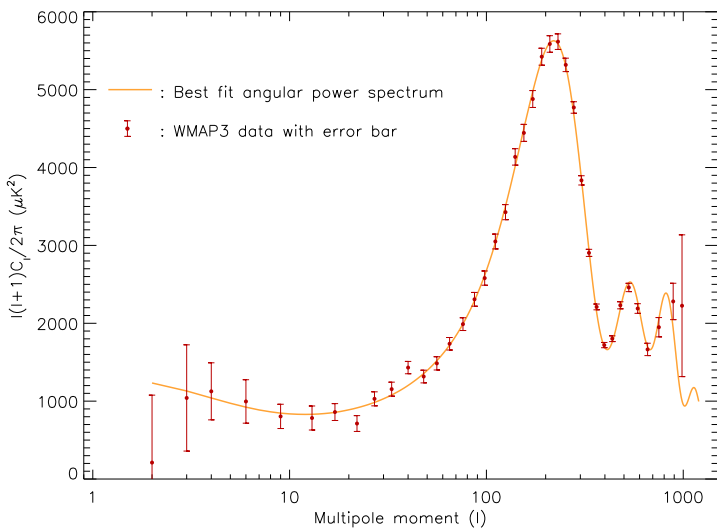
Sound horizon at the photon decoupling epoch  
=  $147 \pm 2$  Mpc (Spergel et al. 2007)

# WMAP 3-year temperature map



3-year ILC Map (Hinshaw et al., 2007)

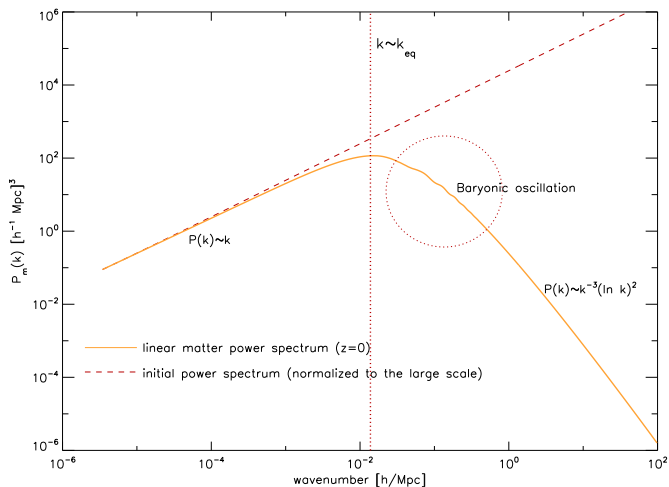
# Triumph of linear perturbation theory



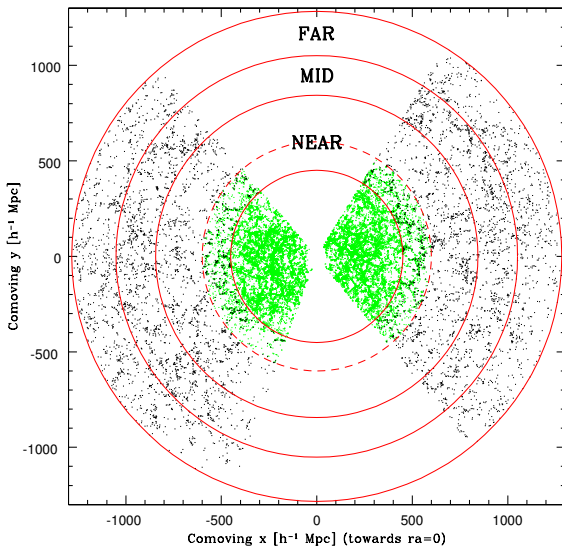
3-year Temperature Power Spectrum (Hinshaw et al. 2007)

**Experimental Verification of the Linear Perturbation Theory!**

# How about the matter $P(k)$ ?

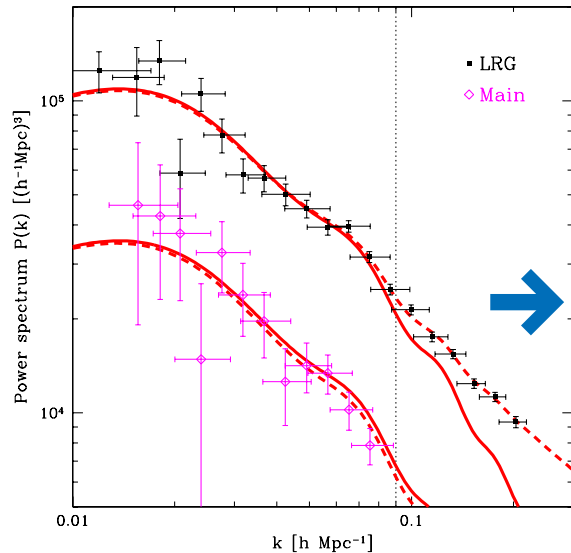


# SDSS Luminous Red Galaxies map ( $z < 0.474$ )



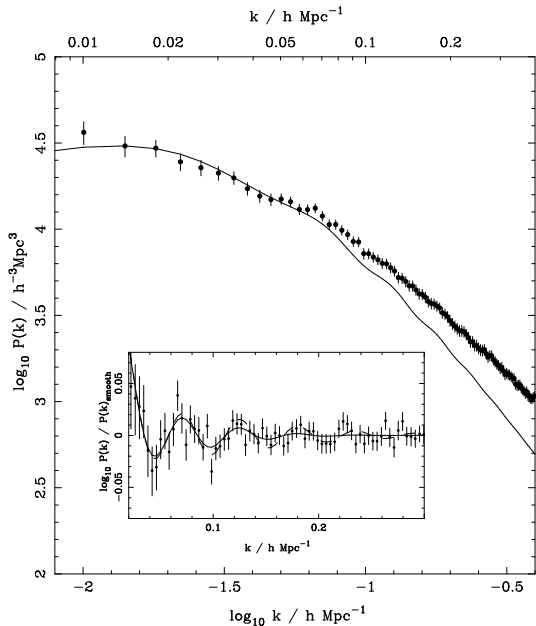
SDSS main galaxies and LRGs (Tegmark et al., 2006)

# SDSS LRG and main galaxy power spectrum



Failure of linear theory is clearly seen.

# BAO from the SDSS power spectrum



The BAOs have been measured in  $P(k)$  successfully (Percival et al. 2006).

The planned galaxy surveys (e.g., HETDEX, WFMOS) will measure BAOs with 10x smaller error bars.

**Is theory ready?**

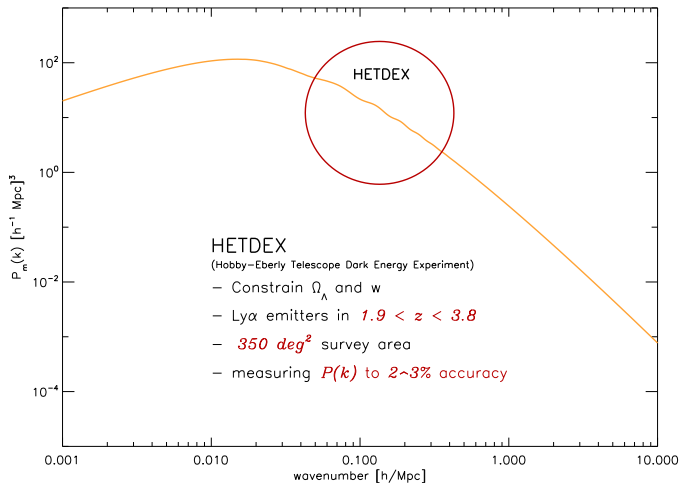
# Systematics: Three Non-linearities

- The SDSS  $P(k)$  has been used only up to  $k < 0.1 hMpc^{-1}$ .
- Why? Non-linearities.
  - **Non-linear evolution of matter clustering**
  - **Non-linear bias**
  - **Non-linear redshift space distortion**
- Can we do better?
  - CMB theory was ready for WMAP's precision measurement.
    - LSS theory has not reached sufficient accuracy.
  - The planned galaxy surveys = *WMAP* for LSS.
    - **Is theory ready?**
  - **The goal:** LSS theory that is ready for precision measurements of  $P(k)$  from the future galaxy surveys.

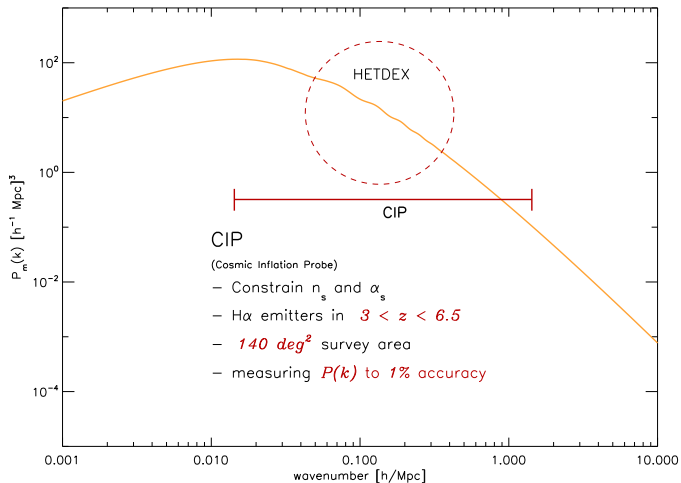
# Our approach: Non-linear perturbation theory

- 3<sup>rd</sup>-order expansion in linear density fluctuations,  $\delta_1$ .  
*c.f.* CMB theory: 1<sup>st</sup>-order (linear) theory.
- Is this approach new? It has been known that non-linear perturbation theory fails at  $z = 0$  ← too non-linear.
- HETDEX ( $z > 2$ ) and CIP ( $z > 3$ ) are at higher- $z$ , where perturbation theory is expected to perform better.

# Upcoming high- $z$ galaxy surveys



# Upcoming high- $z$ galaxy surveys



# Assumptions and basic equations

- Assumptions
  - ① Newtonian matter fluid
  - ② Matter is the pressureless fluid without vorticity.
    - Good approximation before fluctuations go fully non-linear.
    - It is convenient to use the “velocity divergence”,  $\theta = \nabla \cdot \mathbf{v}$
- Equations (Newtonian one component fluid equation)

$$\dot{\delta} + \nabla \cdot [(1 + \delta)\mathbf{v}] = 0$$

$$\dot{\mathbf{v}} + (\mathbf{v} \cdot \nabla) \mathbf{v} = -\frac{\dot{a}}{a} \mathbf{v} - \nabla \phi$$

$$\nabla^2 \phi = 4\pi G a^2 \bar{\rho} \delta$$

- Equations in Fourier space

$$\begin{aligned} & \dot{\delta}(\mathbf{k}, \tau) + \theta(\mathbf{k}, \tau) \\ = & - \int \frac{d^3 k_1}{(2\pi)^3} \int d^3 k_2 \delta_D(\mathbf{k}_1 + \mathbf{k}_2 - \mathbf{k}) \frac{\mathbf{k} \cdot \mathbf{k}_1}{k_1^2} \delta(\mathbf{k}_2, \tau) \theta(\mathbf{k}_1, \tau), \\ & \dot{\theta}(\mathbf{k}, \tau) + \frac{\dot{a}}{a} \theta(\mathbf{k}, \tau) + \frac{3\dot{a}^2}{2a^2} \Omega_m(\tau) \delta(\mathbf{k}, \tau) \\ = & - \int \frac{d^3 k_1}{(2\pi)^3} \int d^3 k_2 \delta_D(\mathbf{k}_1 + \mathbf{k}_2 - \mathbf{k}) \frac{k^2 (\mathbf{k}_1 \cdot \mathbf{k}_2)}{2k_1^2 k_2^2} \theta(\mathbf{k}_1, \tau) \theta(\mathbf{k}_2, \tau) \end{aligned}$$

- Taylor expanding  $\delta$ , and  $\theta$

$$\delta(\mathbf{k}, \tau) = \sum_{n=1}^{\infty} a^n(\tau) \int \frac{d^3 q_1}{(2\pi)^3} \cdots \frac{d^3 q_{n-1}}{(2\pi)^3} \int d^3 q_n \delta_D\left(\sum_{i=1}^n \mathbf{q}_i - \mathbf{k}\right) F_n(\mathbf{q}_1, \mathbf{q}_2, \dots, \mathbf{q}_n) \delta_1(\mathbf{q}_1) \cdots \delta_1(\mathbf{q}_n),$$

$$\theta(\mathbf{k}, \tau) = - \sum_{n=1}^{\infty} \dot{a}(\tau) a^{n-1}(\tau) \int \frac{d^3 q_1}{(2\pi)^3} \cdots \frac{d^3 q_{n-1}}{(2\pi)^3} \int d^3 q_n \delta_D\left(\sum_{i=1}^n \mathbf{q}_i - \mathbf{k}\right) G_n(\mathbf{q}_1, \mathbf{q}_2, \dots, \mathbf{q}_n) \delta_1(\mathbf{q}_1) \cdots \delta_1(\mathbf{q}_n)$$

# Why 3<sup>rd</sup> order?

- $\delta = \delta_1 + \delta_2 + \delta_3$   
where,  $\delta_2 \propto [\delta_1]^2$ ,  $\delta_3 \propto [\delta_1]^3$
- The power spectrum from the higher order density field :

$$\begin{aligned} & (2\pi)^3 P(k) \delta_D(\mathbf{k} + \mathbf{k}') \\ & \equiv \langle \delta(\mathbf{k}, \tau) \delta(\mathbf{k}', \tau) \rangle \\ & = \langle \delta_1(\mathbf{k}, \tau) \delta_1(\mathbf{k}', \tau) \rangle + \langle \delta_2(\mathbf{k}, \tau) \delta_1(\mathbf{k}', \tau) + \delta_1(\mathbf{k}, \tau) \delta_2(\mathbf{k}', \tau) \rangle \\ & \quad + \langle \delta_1(\mathbf{k}, \tau) \delta_3(\mathbf{k}', \tau) + \delta_2(\mathbf{k}, \tau) \delta_2(\mathbf{k}', \tau) + \delta_3(\mathbf{k}, \tau) \delta_1(\mathbf{k}', \tau) \rangle \\ & \quad + \mathcal{O}(\delta_1^6) \end{aligned}$$

- Therefore,  $P(k) = P_{11}(k) + P_{22}(k) + 2P_{13}(k)$

# Why 3<sup>rd</sup> order?

- $\delta = \delta_1 + \delta_2 + \delta_3$   
where,  $\delta_2 \propto [\delta_1]^2$ ,  $\delta_3 \propto [\delta_1]^3$
- The power spectrum from the higher order density field :

$$\begin{aligned} & (2\pi)^3 P(k) \delta_D(\mathbf{k} + \mathbf{k}') \\ & \equiv \langle \delta(\mathbf{k}, \tau) \delta(\mathbf{k}', \tau) \rangle \\ & = \langle \delta_1(\mathbf{k}, \tau) \delta_1(\mathbf{k}', \tau) \rangle + \langle \delta_2(\mathbf{k}, \tau) \delta_1(\mathbf{k}', \tau) + \delta_1(\mathbf{k}, \tau) \delta_2(\mathbf{k}', \tau) \rangle \\ & \quad + \langle \delta_1(\mathbf{k}, \tau) \delta_3(\mathbf{k}', \tau) + \delta_2(\mathbf{k}, \tau) \delta_2(\mathbf{k}', \tau) + \delta_3(\mathbf{k}, \tau) \delta_1(\mathbf{k}', \tau) \rangle \\ & \quad + \mathcal{O}(\delta_1^6) \end{aligned}$$

- Therefore,  $P(k) = P_{11}(k) + P_{22}(k) + 2P_{13}(k)$

# Non-linear matter power spectrum: analytic solution

(Vishniac 1983; Fry 1984; Goroff et al. 1986; Suto & Sasaki 1991; Makino et al. 1992; Jain & Bertschinger 1994; Scoccimarro & Frieman 1996)

$$P_{\delta\delta}(k, \tau) = D^2(\tau)P_L(k) + D^4(\tau) [2P_{13}(k) + P_{22}(k)],$$

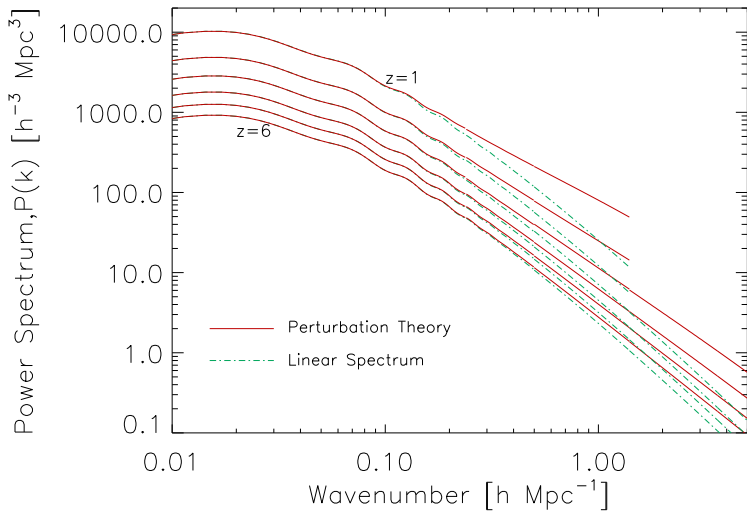
where,

$$P_{22}(k) = 2 \int \frac{d^3q}{(2\pi)^3} P_L(q) P_L(|\mathbf{k} - \mathbf{q}|) \left[ F_2^{(s)}(\mathbf{q}, \mathbf{k} - \mathbf{q}) \right]^2$$

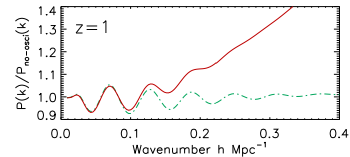
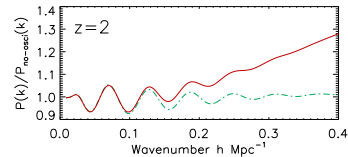
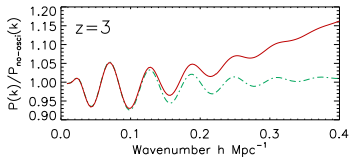
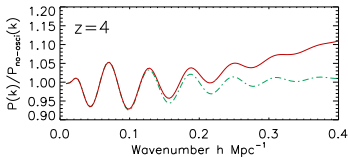
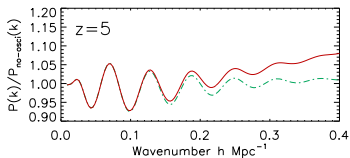
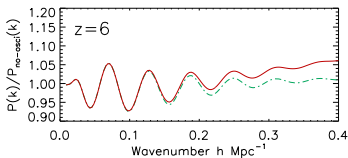
$$\begin{aligned} 2P_{13}(k) &= \frac{2\pi k^2}{252} P_L(k) \int_0^\infty \frac{dq}{(2\pi)^3} P_L(q) \\ &\times \left[ 100 \frac{q^2}{k^2} - 158 + 12 \frac{k^2}{q^2} - 42 \frac{q^4}{k^4} \right. \\ &\left. + \frac{3}{k^5 q^3} (q^2 - k^2)^3 (2k^2 + 7q^2) \ln \left( \frac{k+q}{|k-q|} \right) \right] \end{aligned}$$

$$F_2^{(s)}(\mathbf{q}_1, \mathbf{q}_2) = \frac{17}{21} + \frac{1}{2} \hat{\mathbf{q}}_1 \cdot \hat{\mathbf{q}}_2 \left( \frac{q_1}{q_2} + \frac{q_2}{q_1} \right) + \frac{2}{7} \left[ (\hat{\mathbf{q}}_1 \cdot \hat{\mathbf{q}}_2)^2 - \frac{1}{3} \right]$$

# Prediction: non-linear matter $P(k)$



# Prediction: Baryon Acoustic Oscillations



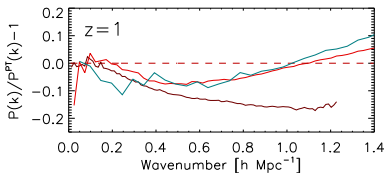
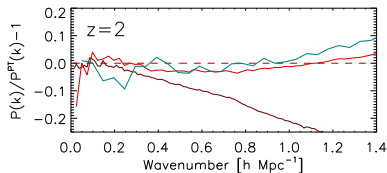
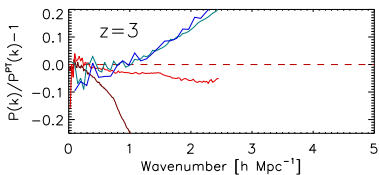
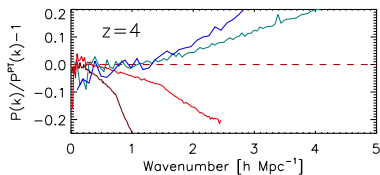
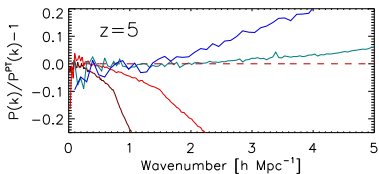
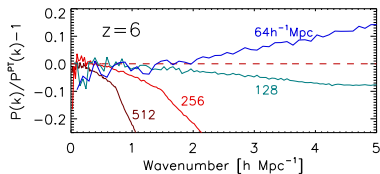
Non-linearity distorts BAOs significantly.

# Simulation Set I: Low-resolution (faster)

- Particle-Mesh (PM) Poisson solver (Ryu et al. 1993)
- Cosmological parameters  
 $\Omega_m = 0.27$ ,  $\Omega_\Lambda = 0.73$ ,  $\Omega_b = 0.043$ ,  
 $H_0 = 70$  km/s/Mpc,  $\sigma_8 = 0.8$ ,  $n_s = 1.0$
- Simulation parameters

Box size [Mpc/h] <sup>3</sup>	$n_{particle}$	$M_{particle}(M_\odot)$	$N_{realizations}$	$k_{max}[h \text{ Mpc}^{-1}]$
512 <sup>3</sup>	256 <sup>3</sup>	$2.22 \times 10^{12}$	60	0.24
256 <sup>3</sup>	256 <sup>3</sup>	$2.78 \times 10^{11}$	50	0.5
128 <sup>3</sup>	256 <sup>3</sup>	$3.47 \times 10^{10}$	20	1.4
64 <sup>3</sup>	256 <sup>3</sup>	$4.34 \times 10^9$	15	5

# Testing convergence with 4 box sizes

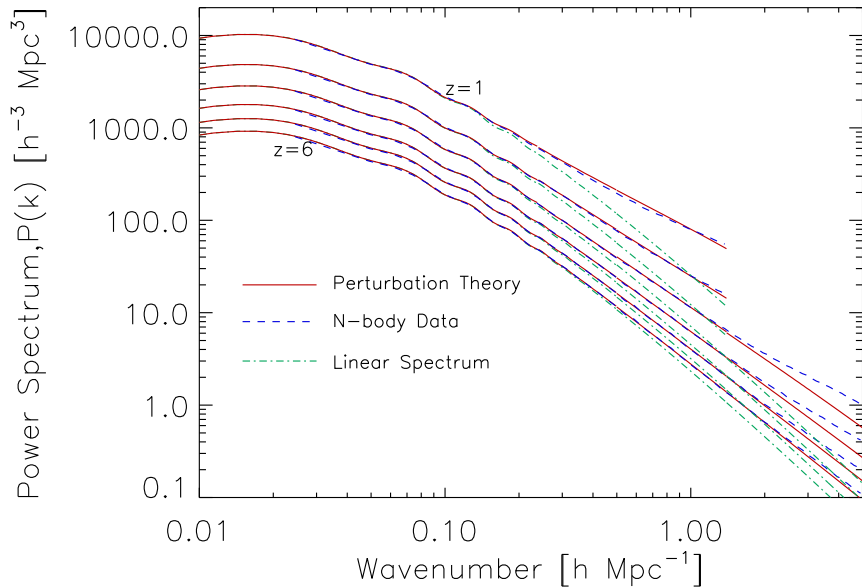


# Simulation Set II: High-resolution

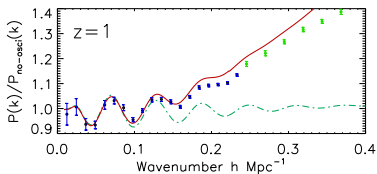
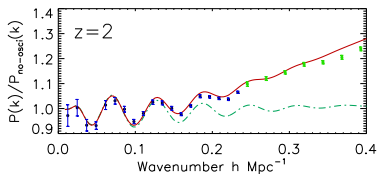
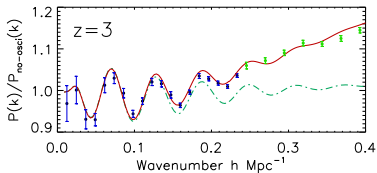
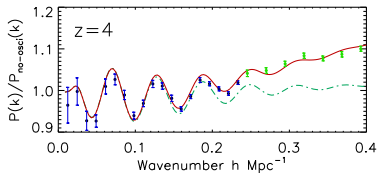
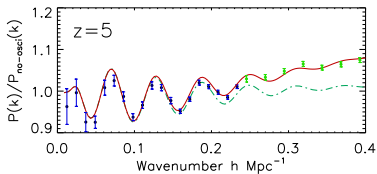
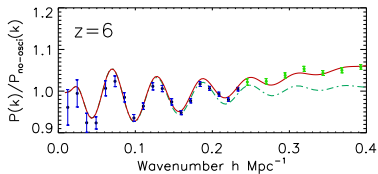
- PMFAST (MPI-parallelized PM) (Merts et al. 2005)
- Cosmological parameters (run1)  
 $\Omega_m = 0.27$ ,  $\Omega_\Lambda = 0.73$ ,  $\Omega_b = 0.044$ ,  
 $H_0 = 70$  km/s/Mpc,  $\sigma_8 = 0.9$ ,  $n_s = 1.0$
- Cosmological parameters (run2)  
 $\Omega_m = 0.27$ ,  $\Omega_\Lambda = 0.73$ ,  $\Omega_b = 0.044$ ,  
 $H_0 = 70$  km/s/Mpc,  $\sigma_8 = 0.8$ ,  $n_s = 0.96$
- Simulation parameters

Box size [Mpc/h] <sup>3</sup>	$n_{particle}$	$M_{particle}(M_\odot)$	$N_{realizations}$
500 <sup>3</sup>	1624 <sup>3</sup>	$8.10 \times 10^9$	1
500 <sup>3</sup>	1624 <sup>3</sup>	$8.10 \times 10^9$	2

# $P(k)$ : Analytical Theory vs Simulations



# BAO: Analytical Theory vs Simulations



## It just works!

(Jeong & Komatsu 2006, ApJ, 651, 619)

A quote from Patrick McDonald (PRD 74, 103512 (2006)):

“  
(...) this perturbative approach to the galaxy power spectrum (including beyond-linear corrections) has not to my knowledge actually been used to interpret real data. However, between improvements in perturbation theory and the need to interpret increasingly precise observations, the time for this kind of approach may have arrived  
”  
(Jeong & Komatsu, 2006).

# From dark matter to halo

- Two Facts
  - i) Galaxies are **biased tracers** of the underlying matter distribution.
  - ii) Galaxies form in dark matter halos.
- How is halo biased?

- Tracers (dark matter halos, galaxies, etc) do not follow the distribution of underlying dark matter density field exactly.
- In linear theory, they differ only by a constant factor, the *linear bias*

$$P_{tracer}(k) = b_1^2 P_m(k).$$

- In non-linear theory, bias is non-linear.
- Working assumption: **The halo formation is a local process.**
- From matter density to halo density (Gaztanaga & Fry 1993)

$$\rho_h(\delta) = \rho_0 + \rho_0' \delta + \frac{1}{2} \rho_0'' \delta^2 + \frac{1}{6} \rho_0''' \delta^3 + \epsilon + \mathcal{O}(\delta_1^4)$$

# The halo power spectrum

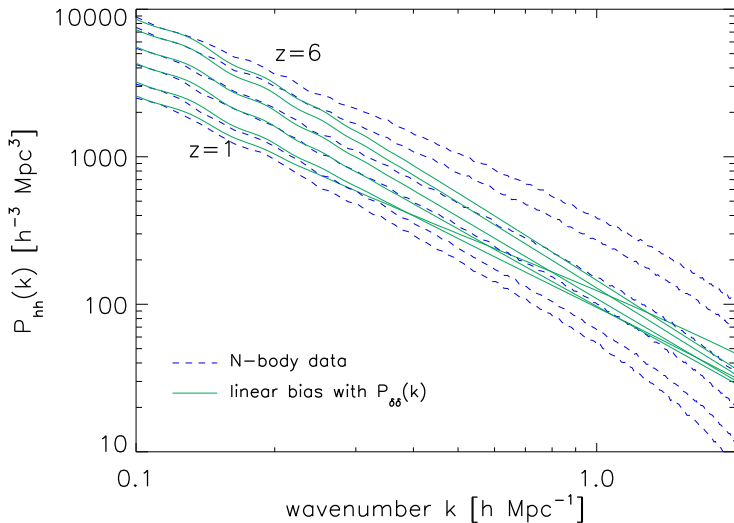
(McDonald 2006)

$$P_{hh}(k) = N + b_1^2 \left[ P(k) + \frac{b_2^2}{2} \int \frac{d^3 \mathbf{q}}{(2\pi)^3} P(q) \left[ P(|\mathbf{k} - \mathbf{q}|) - P(q) \right] \right. \\ \left. + 2b_2 \int \frac{d^3 \mathbf{q}}{(2\pi)^3} P(q) P(|\mathbf{k} - \mathbf{q}|) F_2^{(s)}(\mathbf{q}, \mathbf{k} - \mathbf{q}) \right]$$

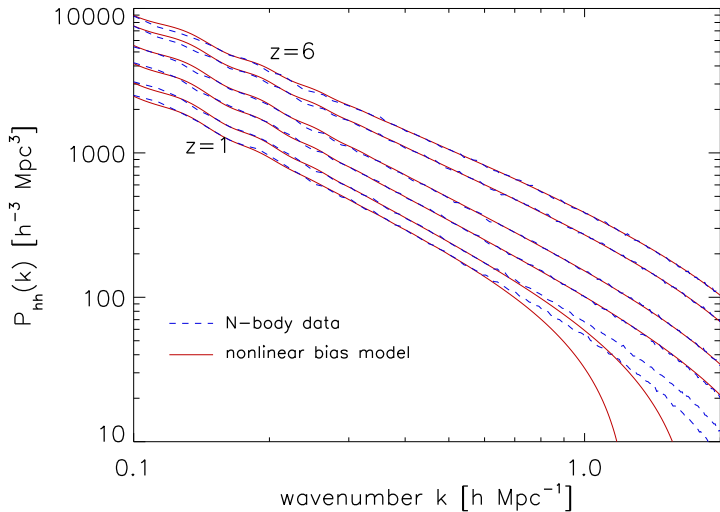
- $b_1$ ,  $b_2$ ,  $N$  are **unknown parameters** that capture detail information on halo formation.
- It is difficult to model them accurately from theory (Smith, Scoccimarro & Sheth 2007).
- Our approach: instead of modeling them, we fit them to match the observed power spectrum.

# Linear Bias Model vs Simulations

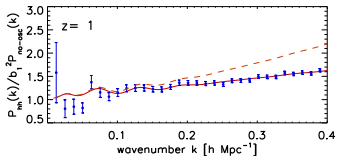
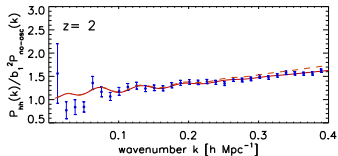
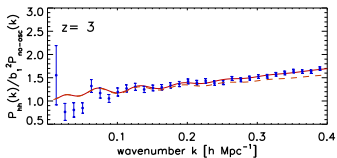
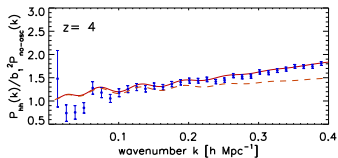
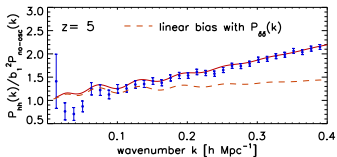
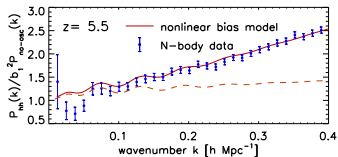
## Linear bias: Horrible!!



# Nonlinear Bias Model vs Simulations



# Effects of Non-linear Bias on BAOs



Non-linear biasing is important even on the BAO scales.

# Best-fit non-linear bias parameters

redshifts	$b_1$	$b_2$	$N$	$N_{shot}$	$k_{max}$ [h/Mpc]
1	1.001	-0.137	3.126	207.191	0.6
2	1.609	0.0996	127.574	234.138	0.6
3	2.468	0.371	371.512	344.949	1.0
4	3.393	0.808	824.337	565.439	2.1
5	4.637	1.563	2215.663	1208.299	2.1
5.5	5.379	2.138	3835.329	1982.772	2.1

- Linear bias  $b_1$  increases with redshift.
- Non-linear bias  $b_2$  also increases with redshift.
- At  $z \sim 1$ , non-linear bias reduces power.
- $N_{shot}$  is a Poisson shot noise given by  $1/n_{halo}$ .
- $k_{max}$  is the wavenumber  $k$  included in the fit that gave  $\chi_{red}^2 \simeq 1$ .

- **Again, it just works.** (Jeong, Komatsu, Iliev & Shapiro, to be submitted)
- **However, it is a 3-parameter fit, and an old-saying says “3 parameters can fit everything.”**
  - *“With four parameters I can fit an elephant, and with five I can make him wiggle his trunk.”* – **John von Neumann.**
- **The important question is, “Can we also extract the correct cosmology?”**

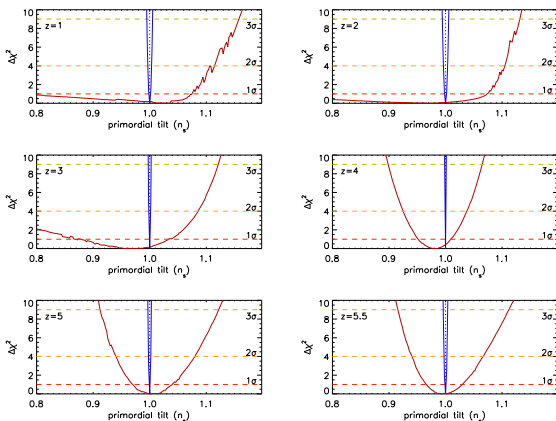
# Example: Shape of the primordial $P(k)$ , $n_s$

## Red curve

Fitting the N-body power spectrum with  $(b_1, b_2, N)$  and  $n_s$ , and marginalize over the bias parameters.

## Blue curve

$\Delta\chi^2$  of  $n_s$  assuming that we know the non-linear bias parameters completely.



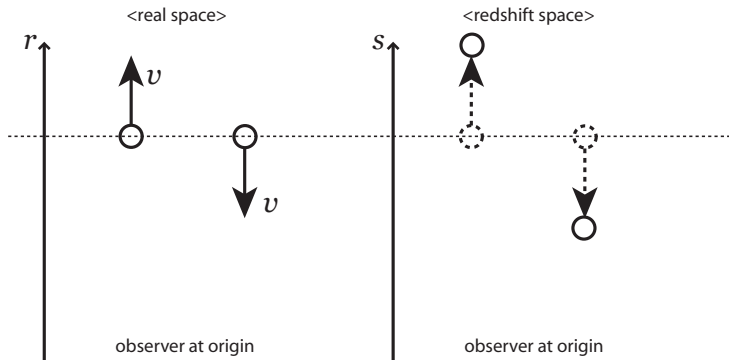
# The Remaining Issue: Redshift Space Distortion

- Redshift space distortion ( $z$ -distortion)
  - To measure  $P(k)$ , we need to measure a density field in 3D position space.
  - We measure the redshift,  $z$ , and calculate the radial separation between galaxies from  $c\Delta z/H(z)$ .
  - This can be done exactly if there is only the Hubble flow.
  - Peculiar motion adds a complication.
  - The peculiar velocity field is not a random field.  
∴ Added correlation must be modeled.

# From real space to redshift space

In a nut shell, redshift space distortion is merely an effect due to the **coordinate transformation**:

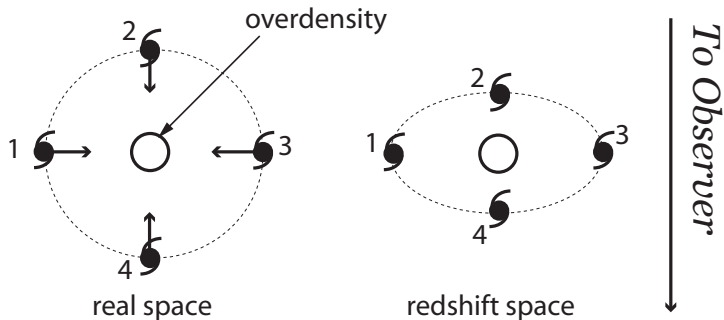
$$\mathbf{s} = \mathbf{r} + \frac{\mathbf{v} \cdot \hat{\mathbf{r}}}{H(z)} \hat{\mathbf{r}} \equiv \mathbf{r} \left[ 1 + \frac{U(\mathbf{r})}{r} \right]$$



# Two effects

- ① Large-scale coherent flow : “Kaiser effect”
- ② Small-scale random motion : “Finger of God effect”

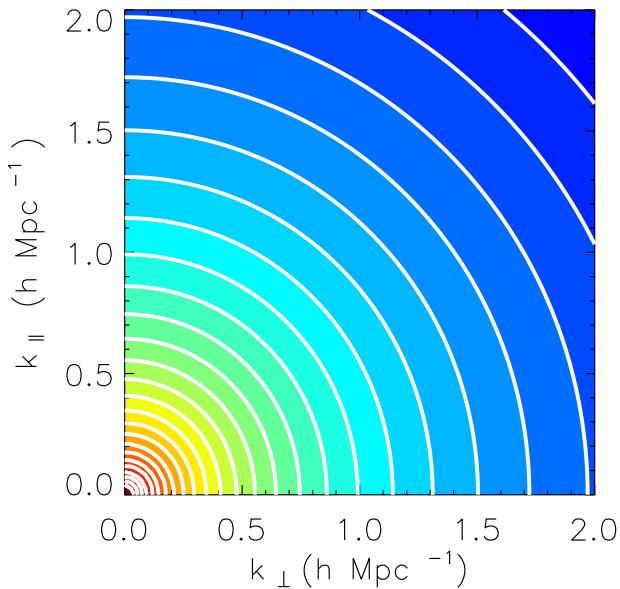
# I. Large scale Kaiser effect



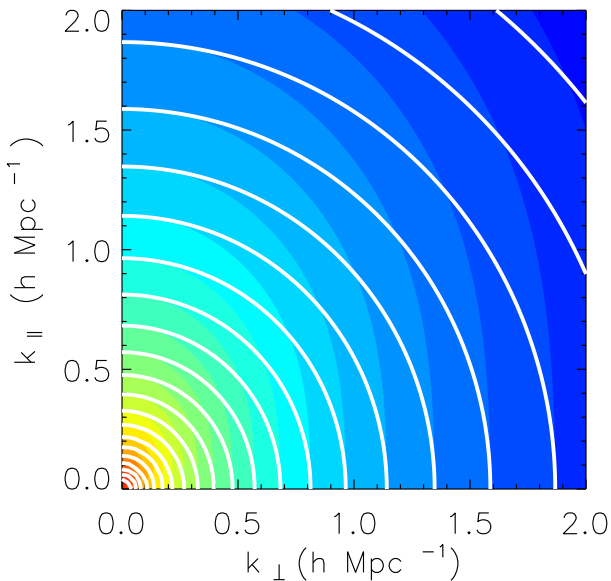
Coherent flow  
towards the  
overdensity

The galaxies along the line of sight appear closer to each other than they actually are. The radial clustering appears stronger. → **increase in power** along the line of sight.

# Real space 2D $P(k_{\perp}, k_{\parallel})$



# Kaiser effect on 2D $P_{red}(k_{\perp}, k_{\parallel})$



# Non-linear Kaiser power spectrum

- Kaiser (1987) is purely linear. We extend it to the 3<sup>rd</sup> order perturbation theory.
- 3<sup>rd</sup>  $P(k)$  in redshift space is given by (Heavens et al. 1998)

$$P(\mathbf{k}) = (1 + f\mu^2)^2 P_{11}(k) + 2 \int \frac{d^3 \mathbf{q}}{(2\pi)^3} P_{11}(q) P_{11}(|\mathbf{k} - \mathbf{q}|) \left[ R_2^{(s)}(\mathbf{q}, \mathbf{k} - \mathbf{q}) \right]^2 \\ + 6(1 + f\mu^2) P_{11}(k) \int \frac{d^3 \mathbf{q}}{(2\pi)^3} P_{11}(q) R_3^{(s)}(\mathbf{q}, -\mathbf{q}, \mathbf{k})$$

- With the following mathematical functions

$$R_1^{(s)}(\mathbf{k}) = 1 + f\mu^2$$

$$R_2^{(s)}(\mathbf{k}_1, \mathbf{k}_2) = F_2^{(s)}(\mathbf{k}_1, \mathbf{k}_2) + f\mu^2 G_2^{(s)}(\mathbf{k}_1, \mathbf{k}_2) \\ + \frac{f}{2} \left[ \mu_1^2 + \mu_2^2 + \mu_1 \mu_2 \left( \frac{k_1}{k_2} + \frac{k_2}{k_1} \right) \right] + f^2 \left[ \mu_1^2 \mu_2^2 + \frac{\mu_1 \mu_2}{2} \left( \mu_1^2 \frac{k_1}{k_2} + \mu_2^2 \frac{k_2}{k_1} \right) \right]$$

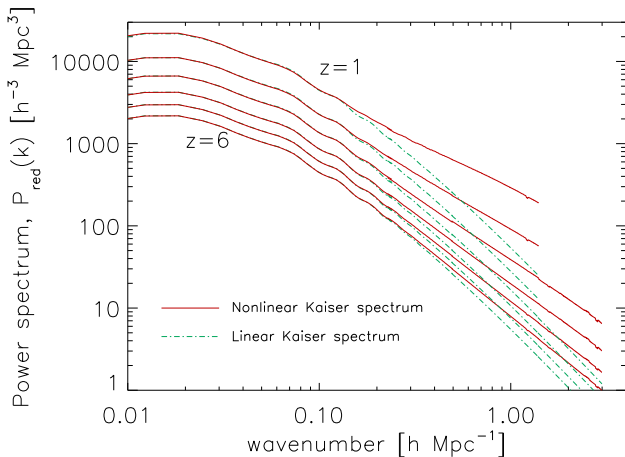
- $\mu$  : cosine of line of sight and  $\mathbf{k}$ .
  - When  $\mu = 0$ ,  $\mathbf{k}$  is perp. to the l.o.s..  
 $P(k)$  agrees with the non-linear matter  $P(k)$  in real space.
  - When  $\mu = 1$ ,  $\mathbf{k}$  is parallel to the l.o.s..

# Non-linear redshift space distortion: $R_3^{(s)}$

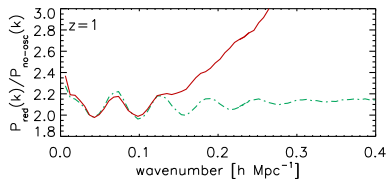
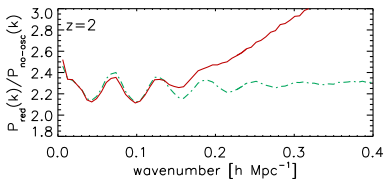
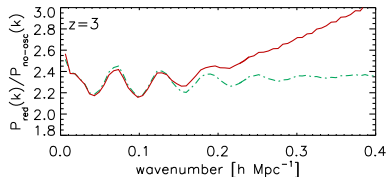
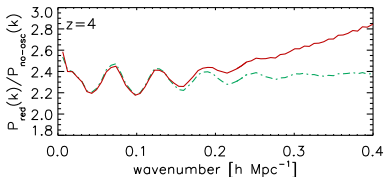
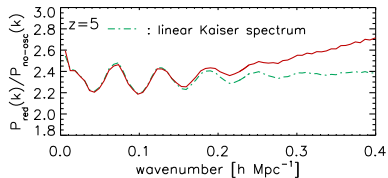
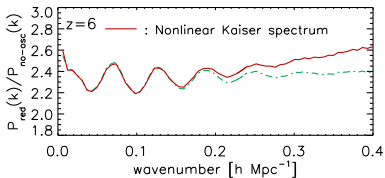
$$\begin{aligned}
 R_3^{(s)}(\mathbf{k}_1, \mathbf{k}_2, \mathbf{k}_3) = & F_3^{(s)}(\mathbf{k}_1, \mathbf{k}_2, \mathbf{k}_3) + f\mu^2 G_3^{(s)}(\mathbf{k}_1, \mathbf{k}_2, \mathbf{k}_3) \\
 & + \frac{f}{3} \left\{ F_2^{(s)}(\mathbf{k}_1, \mathbf{k}_2) \left[ \frac{|\mathbf{k}_1 + \mathbf{k}_2|}{k_3} \mu_3 \mu_{1+2} + \mu_3^2 \right] + F_2^{(s)}(\mathbf{k}_1, \mathbf{k}_3) \left[ \frac{|\mathbf{k}_1 + \mathbf{k}_3|}{k_2} \mu_2 \mu_{1+3} + \mu_2^2 \right] \right. \\
 & \quad \left. + F_2^{(s)}(\mathbf{k}_2, \mathbf{k}_3) \left[ \frac{|\mathbf{k}_2 + \mathbf{k}_3|}{k_1} \mu_1 \mu_{2+3} + \mu_1^2 \right] \right\} \\
 & + \frac{f}{3} \left\{ G_2^{(s)}(\mathbf{k}_1, \mathbf{k}_2) \left[ \frac{k_3}{|\mathbf{k}_1 + \mathbf{k}_2|} \mu_3 \mu_{1+2} + \mu_{1+2}^2 \right] + G_2^{(s)}(\mathbf{k}_1, \mathbf{k}_3) \left[ \frac{k_2}{|\mathbf{k}_1 + \mathbf{k}_3|} \mu_2 \mu_{1+3} + \mu_{1+3}^2 \right] \right. \\
 & \quad \left. + G_2^{(s)}(\mathbf{k}_2, \mathbf{k}_3) \left[ \frac{k_1}{|\mathbf{k}_2 + \mathbf{k}_3|} \mu_1 \mu_{2+3} + \mu_{2+3}^2 \right] \right\} \\
 & + \frac{f^2}{3} \left\{ G_2^{(s)}(\mathbf{k}_1, \mathbf{k}_2) \left[ 2\mu_3^2 \mu_{1+2}^2 + \mu_3 \mu_{1+2} \left( \mu_{1+2}^2 \frac{|\mathbf{k}_1 + \mathbf{k}_2|}{k_3} + \mu_3^2 \frac{k_3}{|\mathbf{k}_1 + \mathbf{k}_2|} \right) \right] \right. \\
 & \quad + G_2^{(s)}(\mathbf{k}_1, \mathbf{k}_3) \left[ 2\mu_2^2 \mu_{1+3}^2 + \mu_2 \mu_{1+3} \left( \mu_{1+3}^2 \frac{|\mathbf{k}_1 + \mathbf{k}_3|}{k_2} + \mu_2^2 \frac{k_2}{|\mathbf{k}_1 + \mathbf{k}_3|} \right) \right] \\
 & \quad \left. + G_2^{(s)}(\mathbf{k}_2, \mathbf{k}_3) \left[ 2\mu_1^2 \mu_{2+3}^2 + \mu_1 \mu_{2+3} \left( \mu_{2+3}^2 \frac{|\mathbf{k}_2 + \mathbf{k}_3|}{k_1} + \mu_1^2 \frac{k_1}{|\mathbf{k}_2 + \mathbf{k}_3|} \right) \right] \right\} \\
 & + f^2 \left\{ \frac{\mu_1 \mu_2 \mu_3}{3} \left[ \mu_3 \left( \frac{k_2}{k_1} + \frac{k_1}{k_2} + \frac{k_3^2}{2k_1 k_2} \right) + \mu_2 \left( \frac{k_1}{k_3} + \frac{k_3}{k_1} + \frac{k_2^2}{2k_3 k_1} \right) + \mu_1 \left( \frac{k_3}{k_2} + \frac{k_2}{k_3} + \frac{k_1^2}{2k_2 k_3} \right) \right] \right. \\
 & \quad + \frac{1}{3} \left( \mu_2^2 \mu_3^2 + \mu_1^2 \mu_3^2 + \mu_1^2 \mu_2^2 \right) \\
 & \quad \left. + \frac{1}{6} \left( \mu_1 \mu_3^3 \frac{k_3}{k_1} + \mu_3 \mu_1^3 \frac{k_1}{k_3} + \mu_1 \mu_2^3 \frac{k_2}{k_1} + \mu_2 \mu_1^3 \frac{k_1}{k_2} + \mu_2 \mu_3^3 \frac{k_3}{k_2} + \mu_3 \mu_2^3 \frac{k_2}{k_3} \right) \right\} \\
 & + f^3 \left\{ \mu_1^2 \mu_2^2 \mu_3^2 + \mu_1 \mu_2 \mu_3 \left[ \frac{1}{3} \left( \mu_3^3 \frac{k_3^2}{2k_1 k_2} + \mu_2^3 \frac{k_2^2}{2k_3 k_1} + \mu_1^3 \frac{k_1^2}{2k_2 k_3} \right) \right] \right. \\
 & \quad \left. + \frac{1}{2} \left( \mu_2 \mu_3^2 \frac{k_3}{k_1} + \mu_1 \mu_3^2 \frac{k_3}{k_2} + \mu_3 \mu_2^2 \frac{k_2}{k_1} + \mu_1 \mu_2^2 \frac{k_2}{k_3} + \mu_3 \mu_1^2 \frac{k_1}{k_2} + \mu_2 \mu_1^2 \frac{k_1}{k_3} \right) \right\}
 \end{aligned}$$

All but the first term disappear when  $\mu = 0$ .

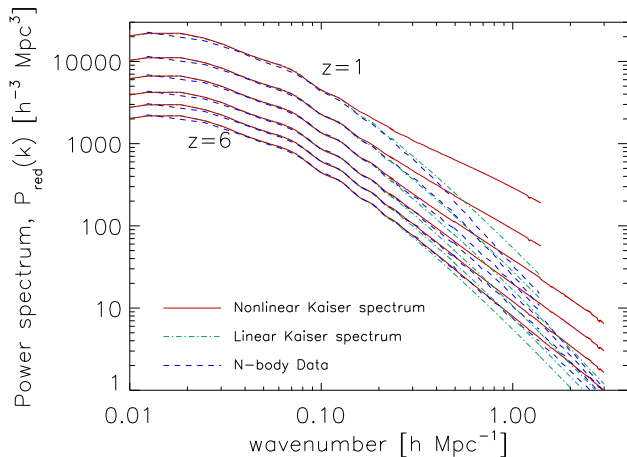
# Prediction: Non-linear Kaiser matter power spectrum



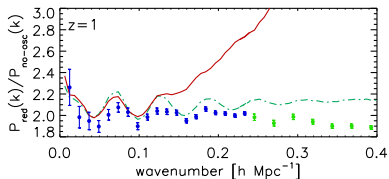
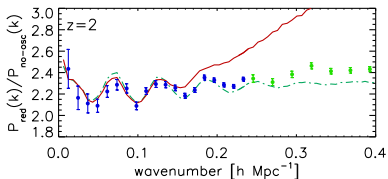
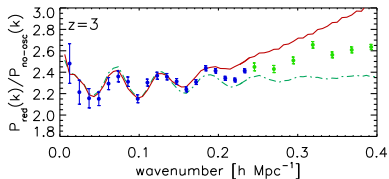
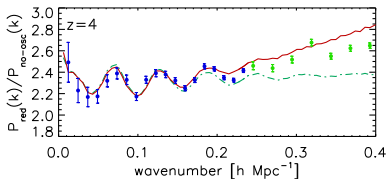
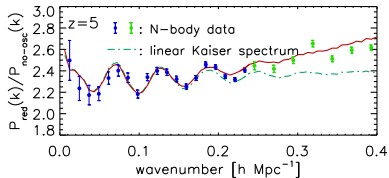
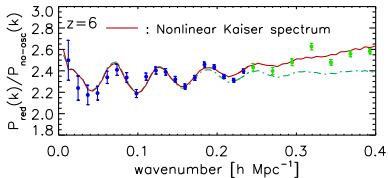
# BAO in redshift space: non-linear Kaiser boost



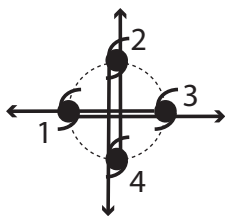
# Non-linear Kaiser vs Simulations: An Issue?



# Simulated BAOs in redshift space: Power Suppression

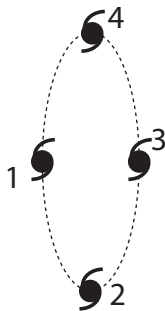


## II. Small scale Finger of God effect



real space

Virial motion in halo



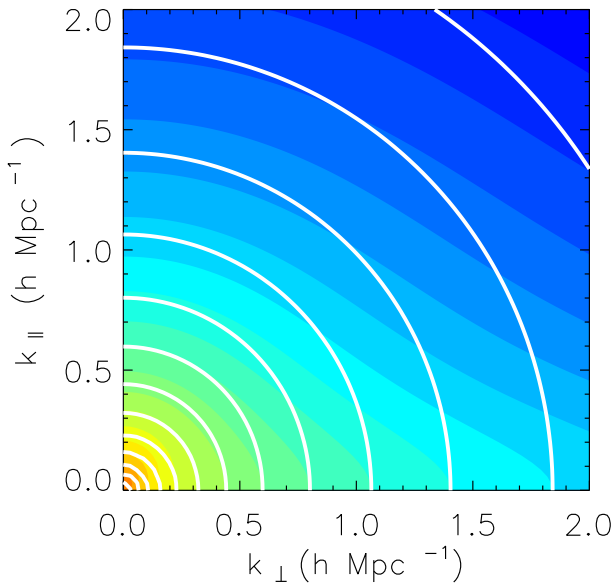
redshift space

*To Observer*



Now, galaxy 2 and 4 are farther away from each other than they actually are. → **suppression of power** along the line of sight.

# FoG effect on 2D $P_{red}(k_{\perp}, k_{\parallel})$



- How can we model the FoG effect?

We have to know **the velocity distribution within halos.**

- Is it a Gaussian? (Peacock 1992)

$$e^{-k_{\parallel}^2 \sigma_v^2}$$

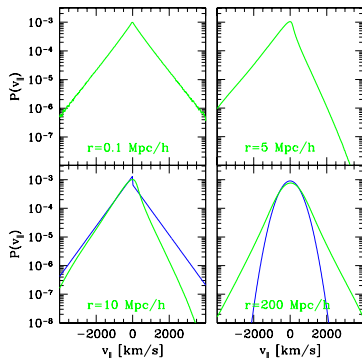
- A better approximation (Ballinger, Peacock & Heavens 1996)

$$1/(1 + k_{\parallel}^2 \sigma_v^2)$$

which corresponds to an exponential velocity distribution.

# L.o.s. velocity distribution is close to exponential than Gaussian

Line of sight velocity distribution calculated from N-body simulations.  
(Scoccimarro, 2004)



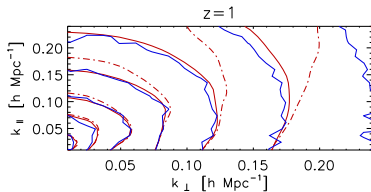
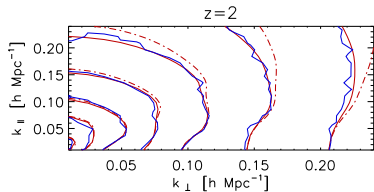
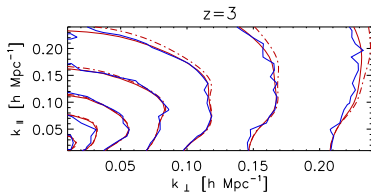
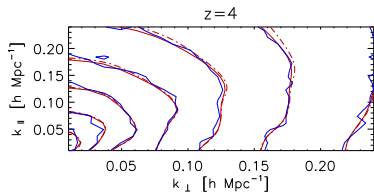
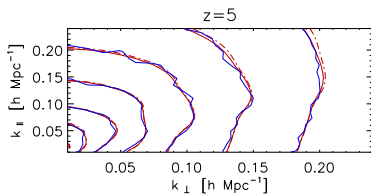
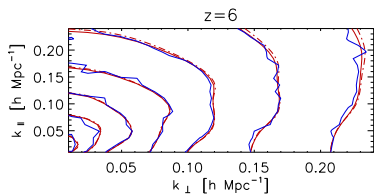
Ansatz:

$$P_{red}(k_{\parallel}, k_{\perp}, z) \longrightarrow \frac{P_{red}(k_{\parallel}, k_{\perp}, z)}{1 + k_{\parallel}^2 \sigma_v^2}$$

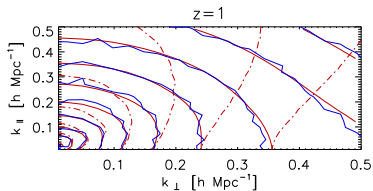
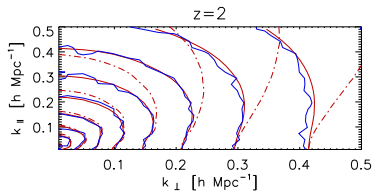
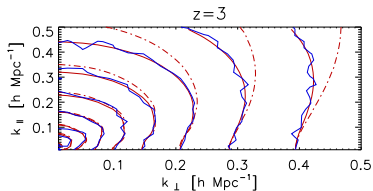
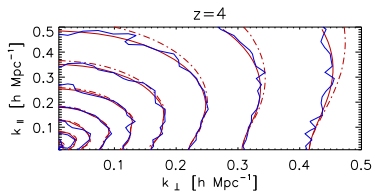
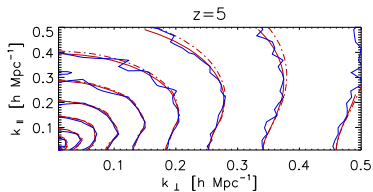
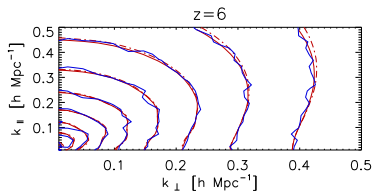
## A Historical Note

An exponential velocity distribution being a better description than a Gaussian has been found for the first time by Peebles (1976) and confirmed by Davis and Peebles (1983).

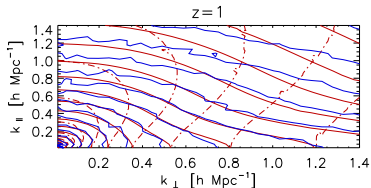
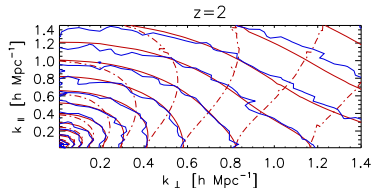
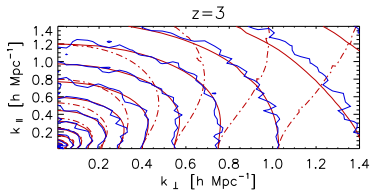
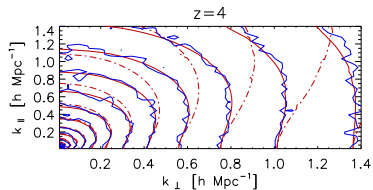
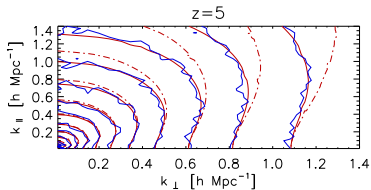
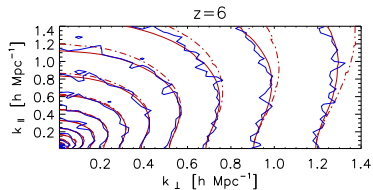
# 2D $P(k)$ in redshift space, $512 h^{-1}$ Mpc box



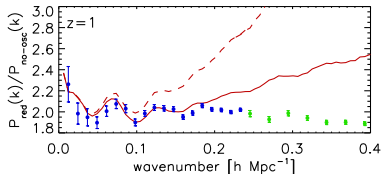
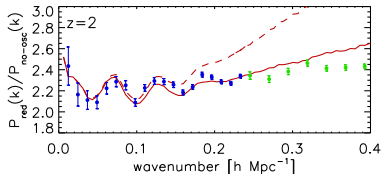
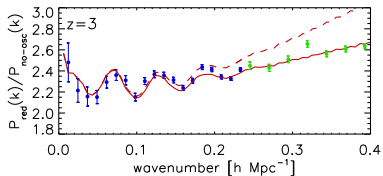
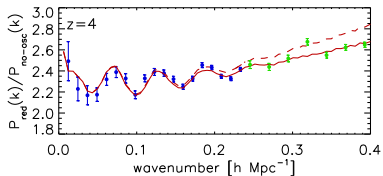
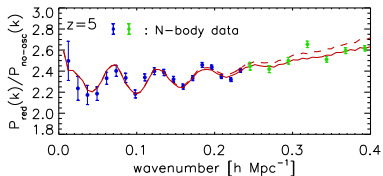
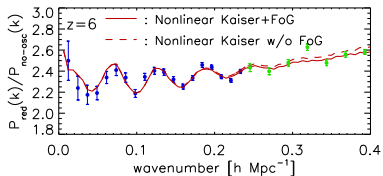
# 2D $P(k)$ in redshift space, $256 h^{-1}$ Mpc box



# 2D $P(k)$ in redshift space, $128 h^{-1}$ Mpc box



# BAOs in Redshift Space with FoG vs Simulations



# Best-fit $\sigma_v^2$ parameters

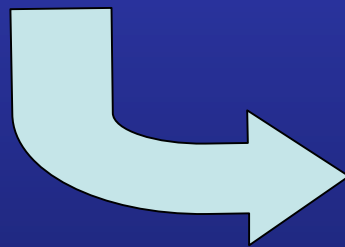
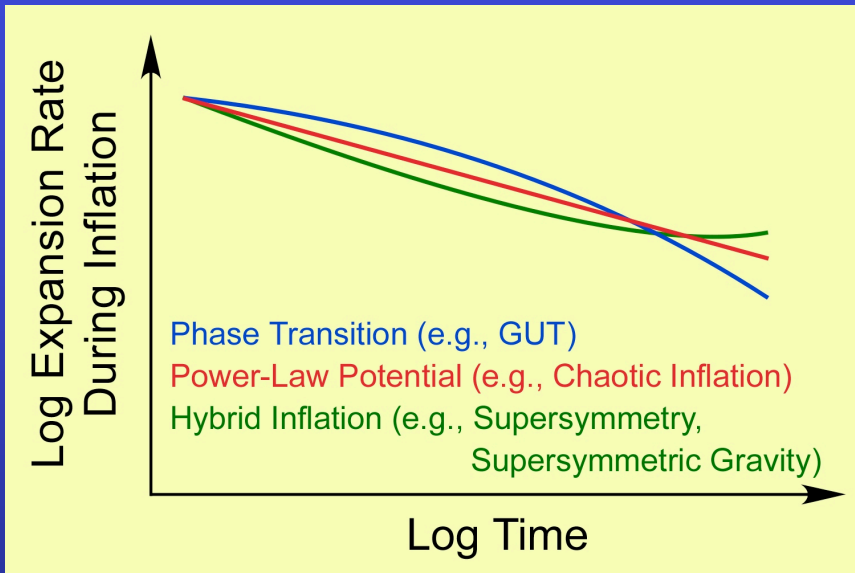
redshift	k-range (h/Mpc)	$\sigma_v^2$ (Eq.56) [Mpc/h] <sup>2</sup>	$\sigma_v^2$ fit [Mpc/h] <sup>2</sup>	$\chi_{red}^2$	d.o.f.
6	$k < 0.24$	1.1530	0.4964±0.1151	1.102	318
	$k < 0.5$	1.1686	0.1769±0.0279	1.152	345
	$k < 1.4$	1.1574	0.1009±0.0034	1.580	667
5	$k < 0.24$	1.5778	0.6096±0.1156	1.091	318
	$k < 0.5$	1.5989	0.3013±0.0284	1.149	345
	$k < 1.4$	1.5832	0.2166±0.0039	1.502	667
4	$k < 0.24$	2.2427	0.8306±0.1171	1.086	318
	$k < 0.5$	2.2707	0.5895±0.0294	1.144	345
	$k < 1.4$	2.2506	0.5155±0.0049	1.411	667
3	$k < 0.24$	3.5667	1.3945±0.1205	1.079	318
	$k < 0.5$	3.4785	1.4445±0.0333	1.155	345
	$k < 1.2$	3.5427	1.5606±0.0118	1.442	494
2	$k < 0.24$	6.0760	3.4408±0.1338	1.144	318
	$k < 0.33$	6.1519	4.2194±0.1553	1.053	154
	$k < 1.4$	6.0887	5.0000±0.0167	2.431	667
1	$k < 0.15$	12.8654	10.2650±0.8443	1.149	131
	$k < 0.5$	12.6851	19.8754±0.0975	2.292	345
	$k < 1.4$	12.6543	23.8262±0.0598	10.335	667

What science can we do with the planned high- $z$  galaxy surveys, coupled with the accurate theoretical predictions that we have presented?

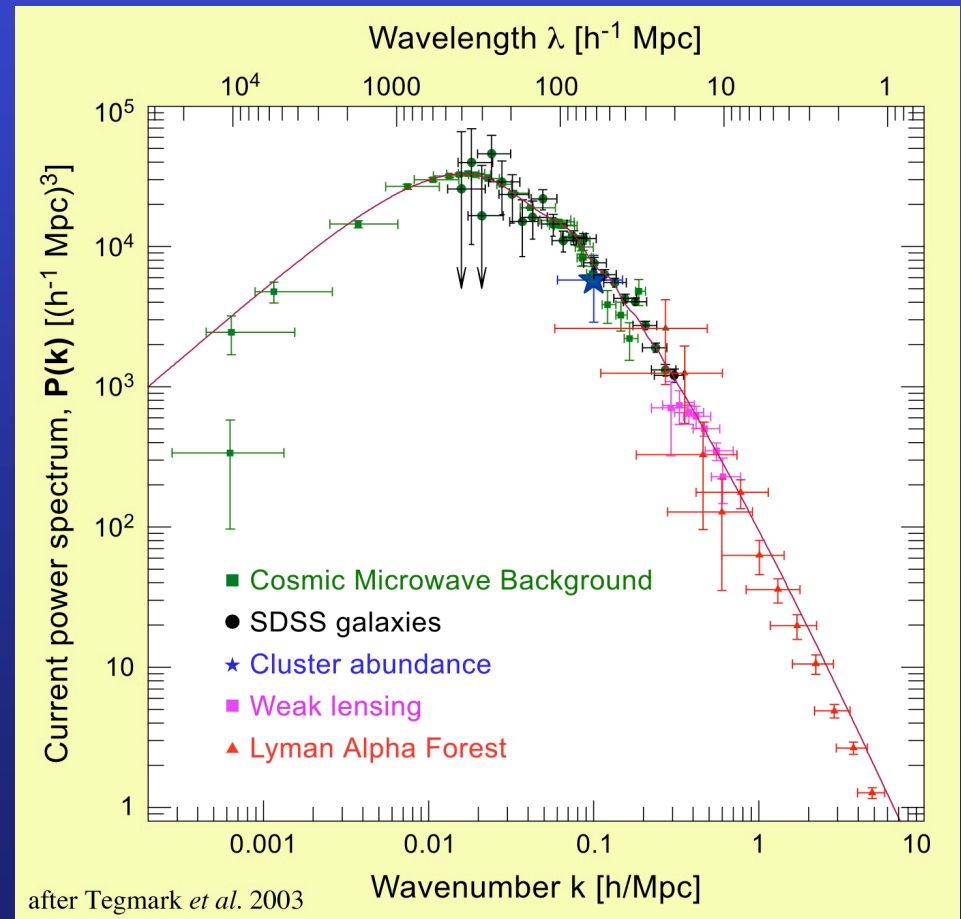
- Nature of dark energy
- Physics of Inflation
- Neutrino Mass

to mention a few.

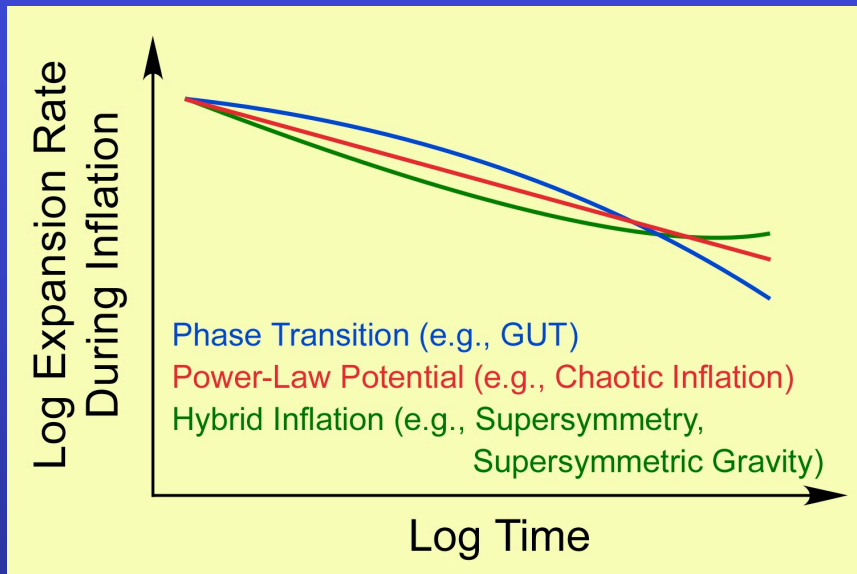
# Expansion history determines structure



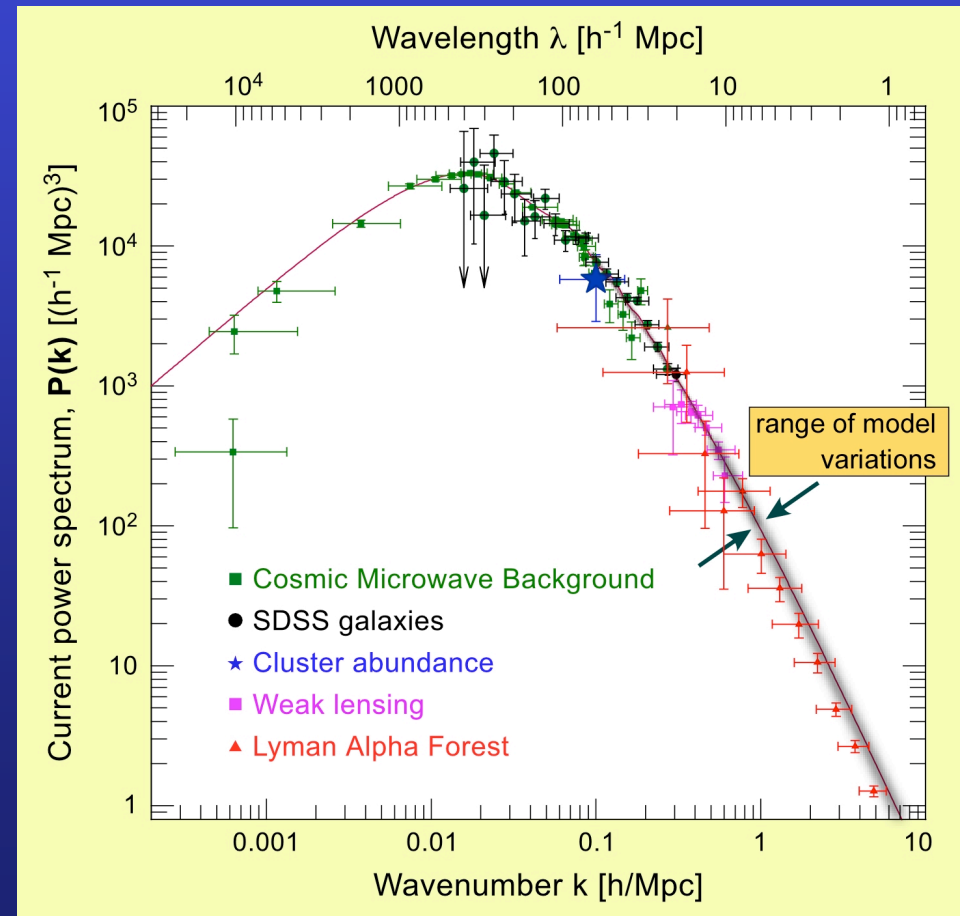
Power Spectrum:  
Relative structure on various size scales



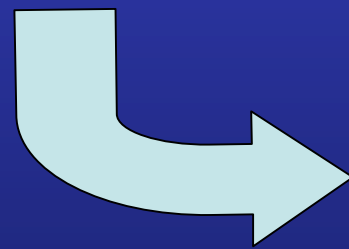
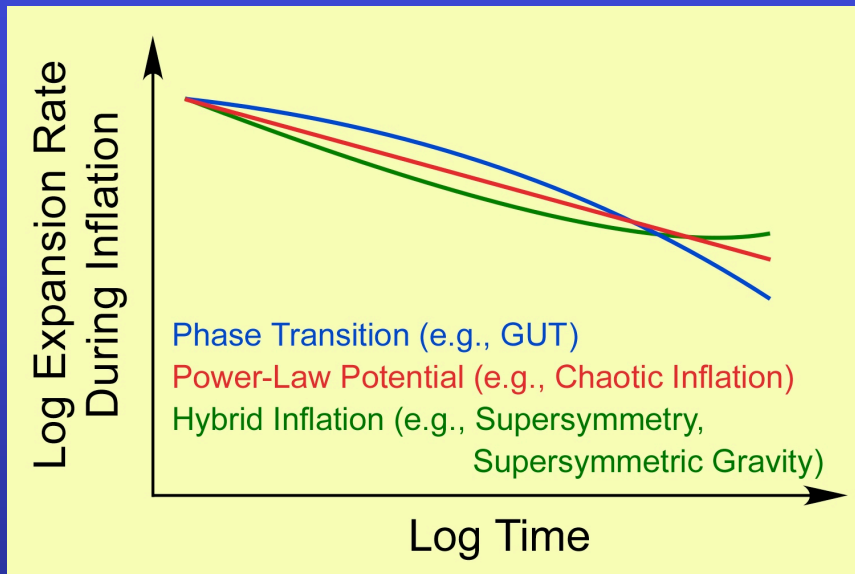
# Expansion history determines structure



Models produce similar, but distinct, Power Spectra  
Need < few % measurement accuracy



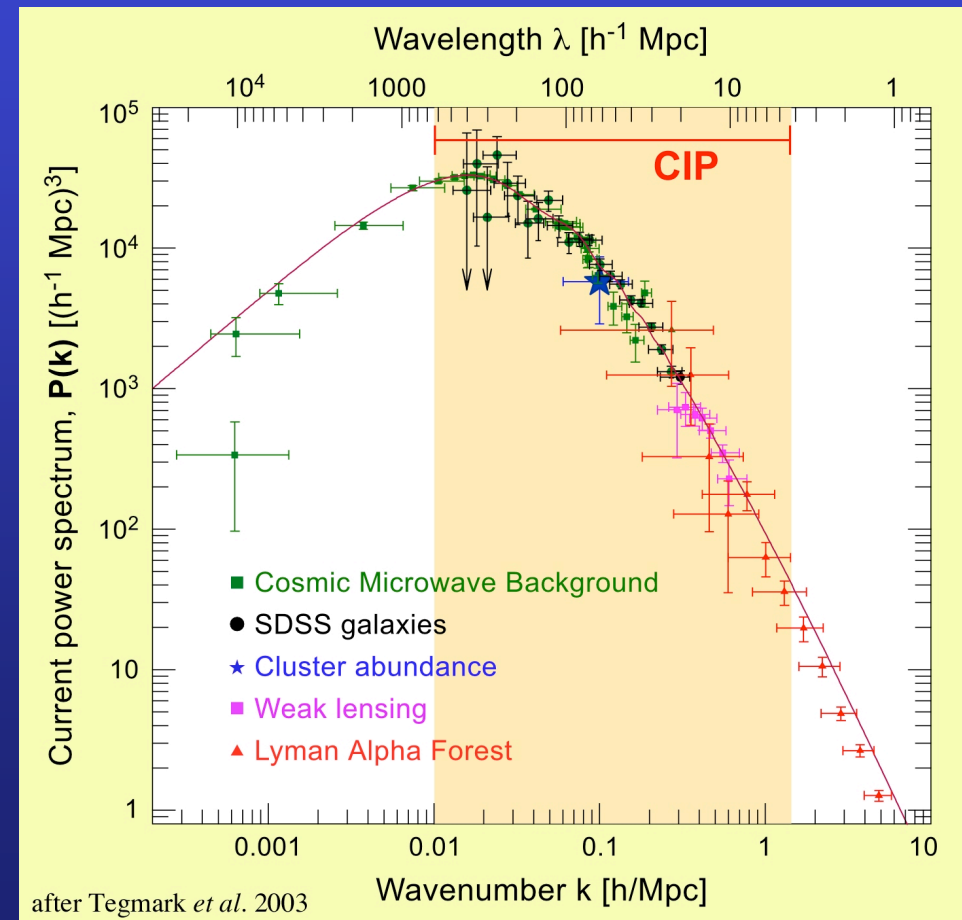
# Expansion history determines structure



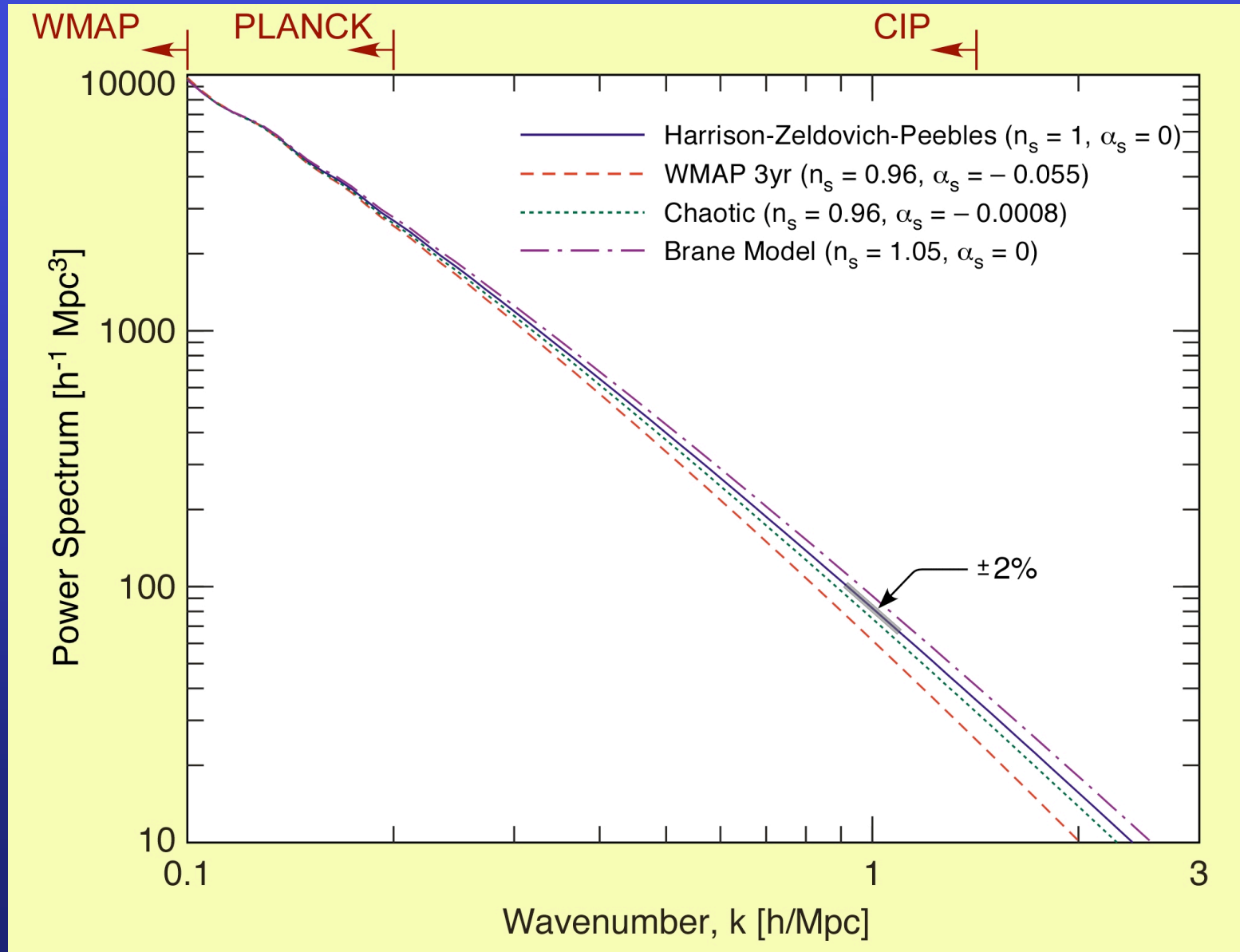
Models produce similar, but distinct, Power Spectra

Need < few % measurement accuracy

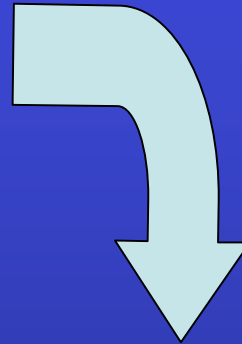
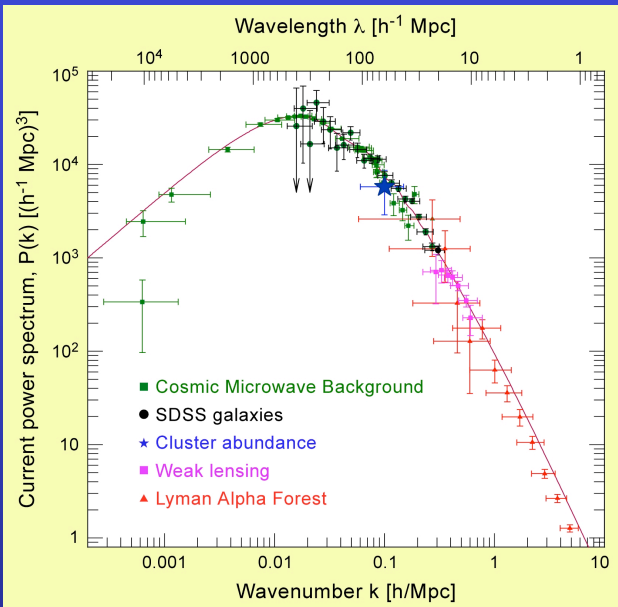
*CIP will measure the Power Spectrum with an accuracy of ~ 1%*



# Expansion history determines structure



# Shape of the Power Spectrum constrains Inflation



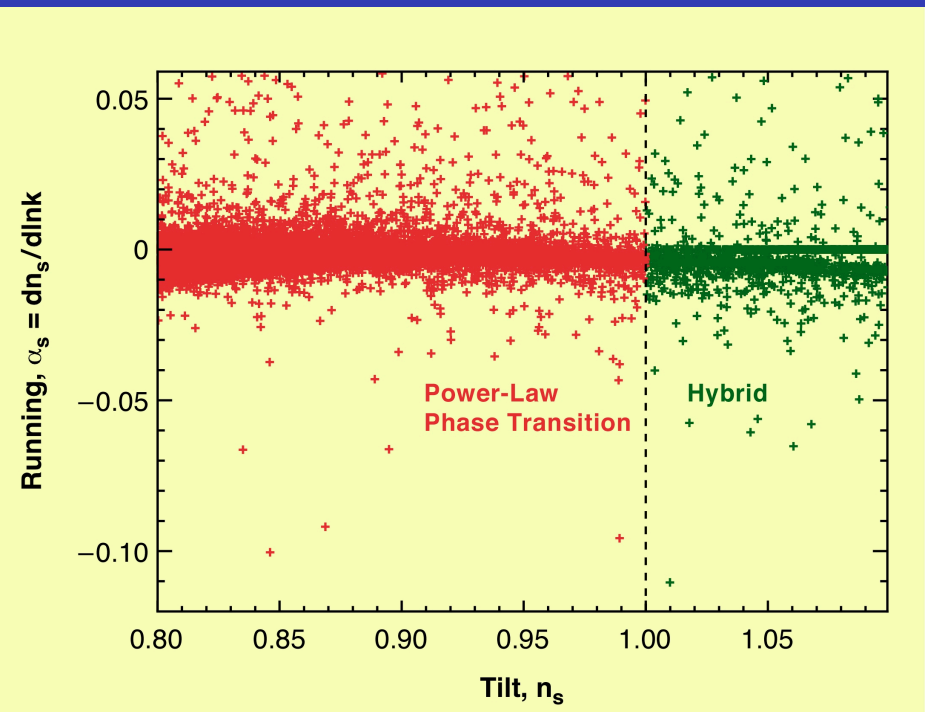
Values of “running” and  
“tilt” predicted by all  
current single scalar field  
Inflation models

Inflation predicts a *nearly* power-law  
primordial power spectrum:

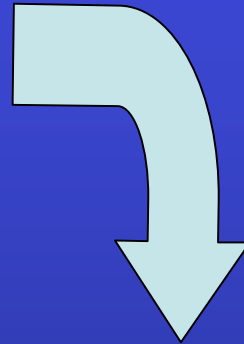
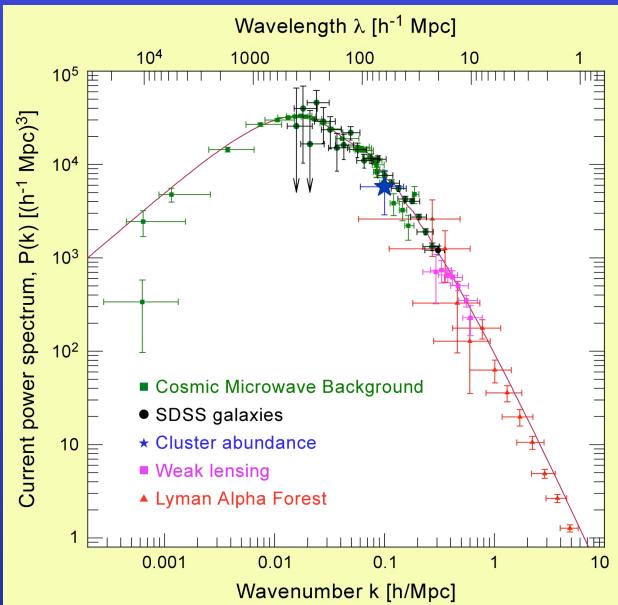
$$P_{prim}(k) = A \left( \frac{k}{k_0} \right)^{n_s - 1 + \frac{1}{2} \alpha_s \ln \left( \frac{k}{k_0} \right)}$$

$n_s$ : power-law index, “tilt”

$\alpha_s$ : deviation from a power-law, “running”



# Shape of the Power Spectrum constrains Inflation



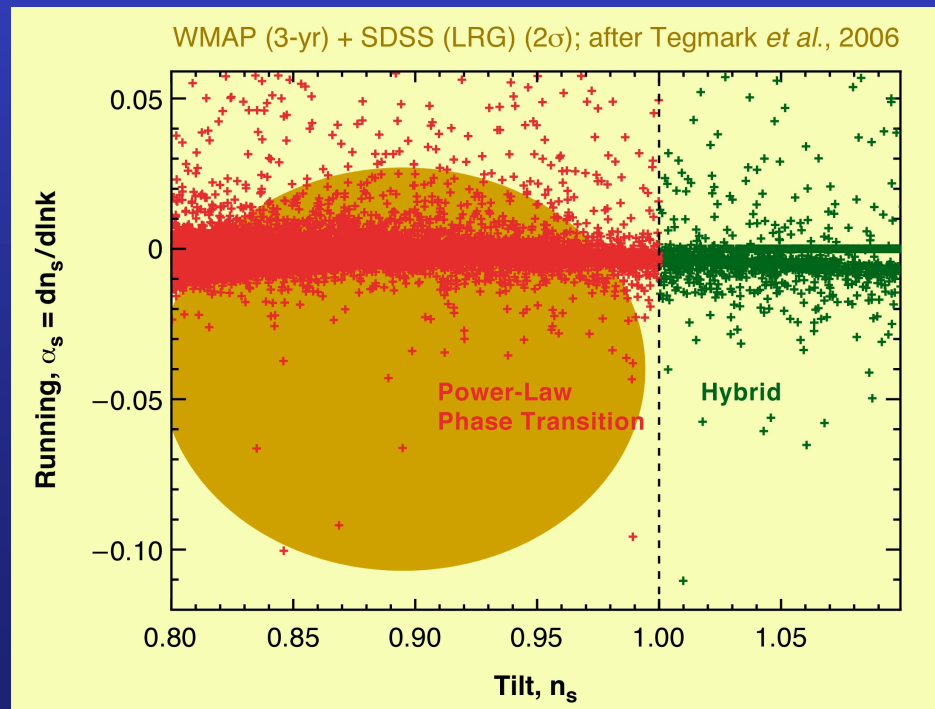
WMAP (3-yr) + SDSS (LRG) observations have narrowed the range of acceptable values

Inflation predicts a *nearly* power-law primordial power spectrum:

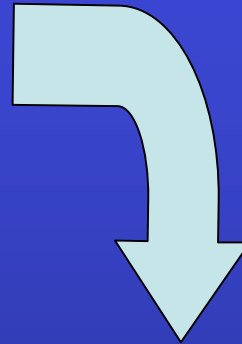
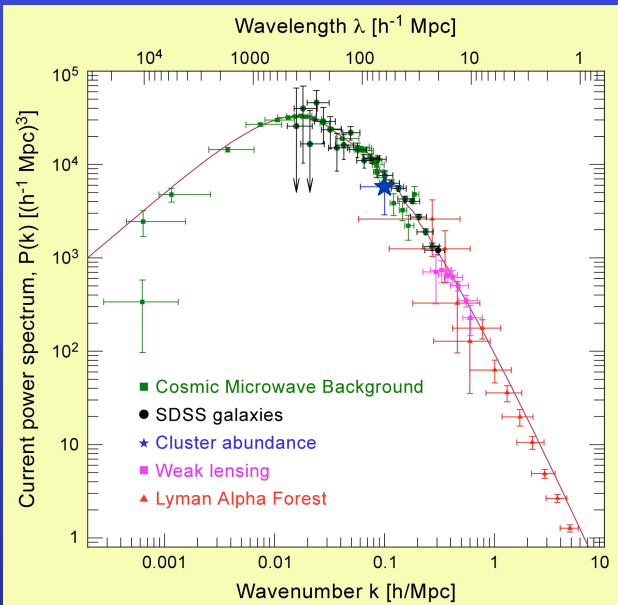
$$P_{prim}(k) = A \left( \frac{k}{k_0} \right)^{n_s - 1 + \frac{1}{2} \alpha_s \ln \left( \frac{k}{k_0} \right)}$$

$n_s$ : power-law index, “tilt”

$\alpha_s$ : deviation from a power-law, “running”



# Shape of the Power Spectrum constrains Inflation



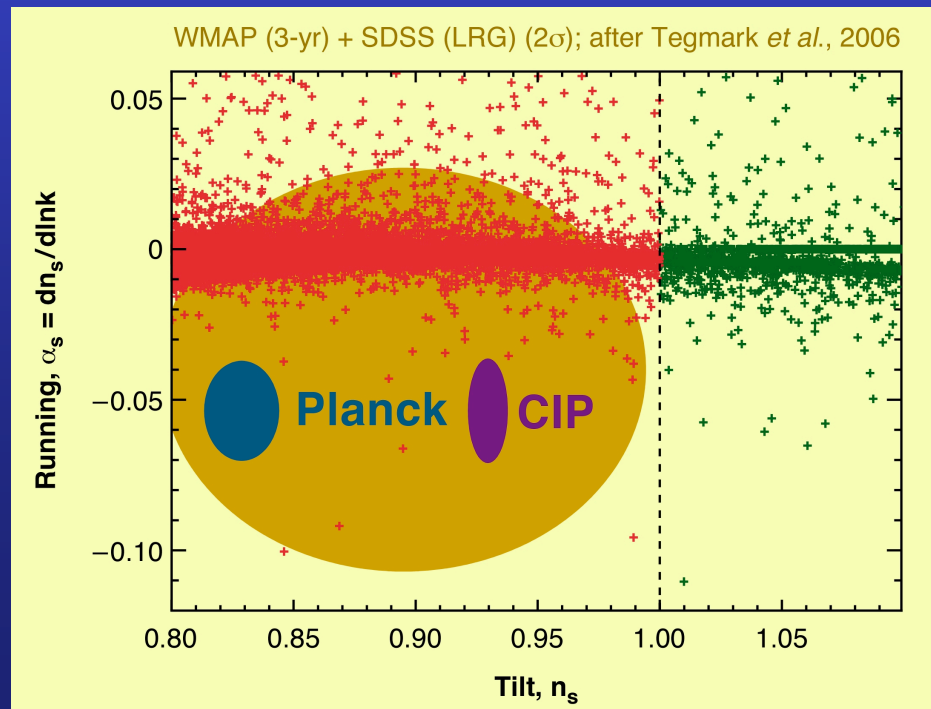
Planck and CIP will achieve comparable  $2\sigma$  limits on  $n_s$  and  $\alpha_s$ , BUT AT SIGNIFICANTLY DIFFERENT  $k$  ranges

Inflation predicts a *nearly* power-law primordial power spectrum:

$$P_{prim}(k) = A \left( \frac{k}{k_0} \right)^{n_s - 1 + \frac{1}{2} \alpha_s \ln \left( \frac{k}{k_0} \right)}$$

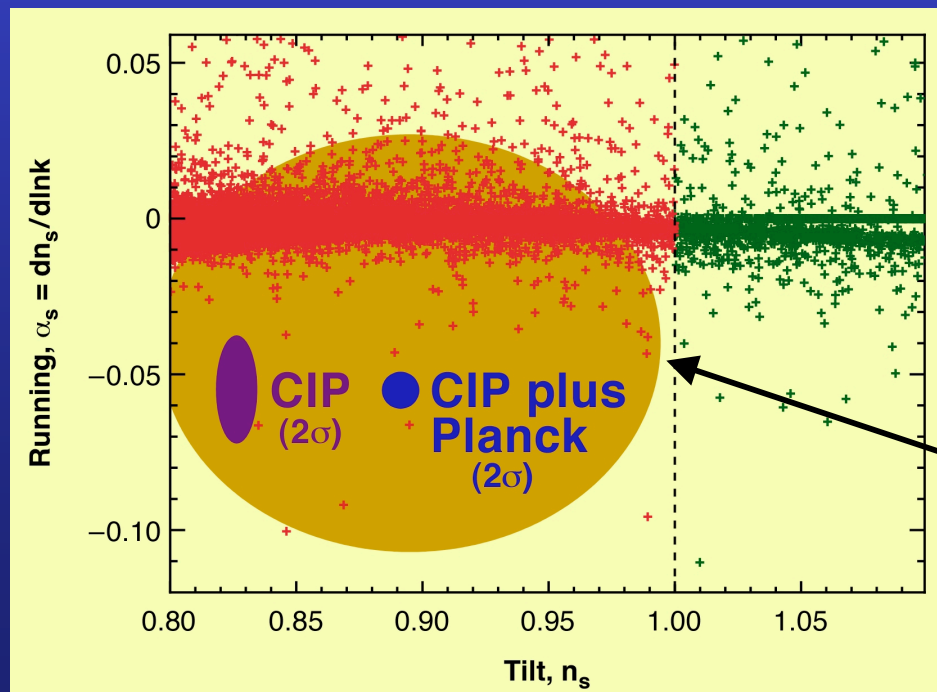
$n_s$ : power-law index, “tilt”

$\alpha_s$ : deviation from a power-law, “running”



# Shape of the Power Spectrum Constrains Inflation

- CIP, alone, can measure the Power Spectrum on small spatial scales with sufficient accuracy to greatly improve constraints on Inflation models
- Combining CIP with CMB measurements samples the broadest range of spatial scales and sets the tightest constraints on Inflation models

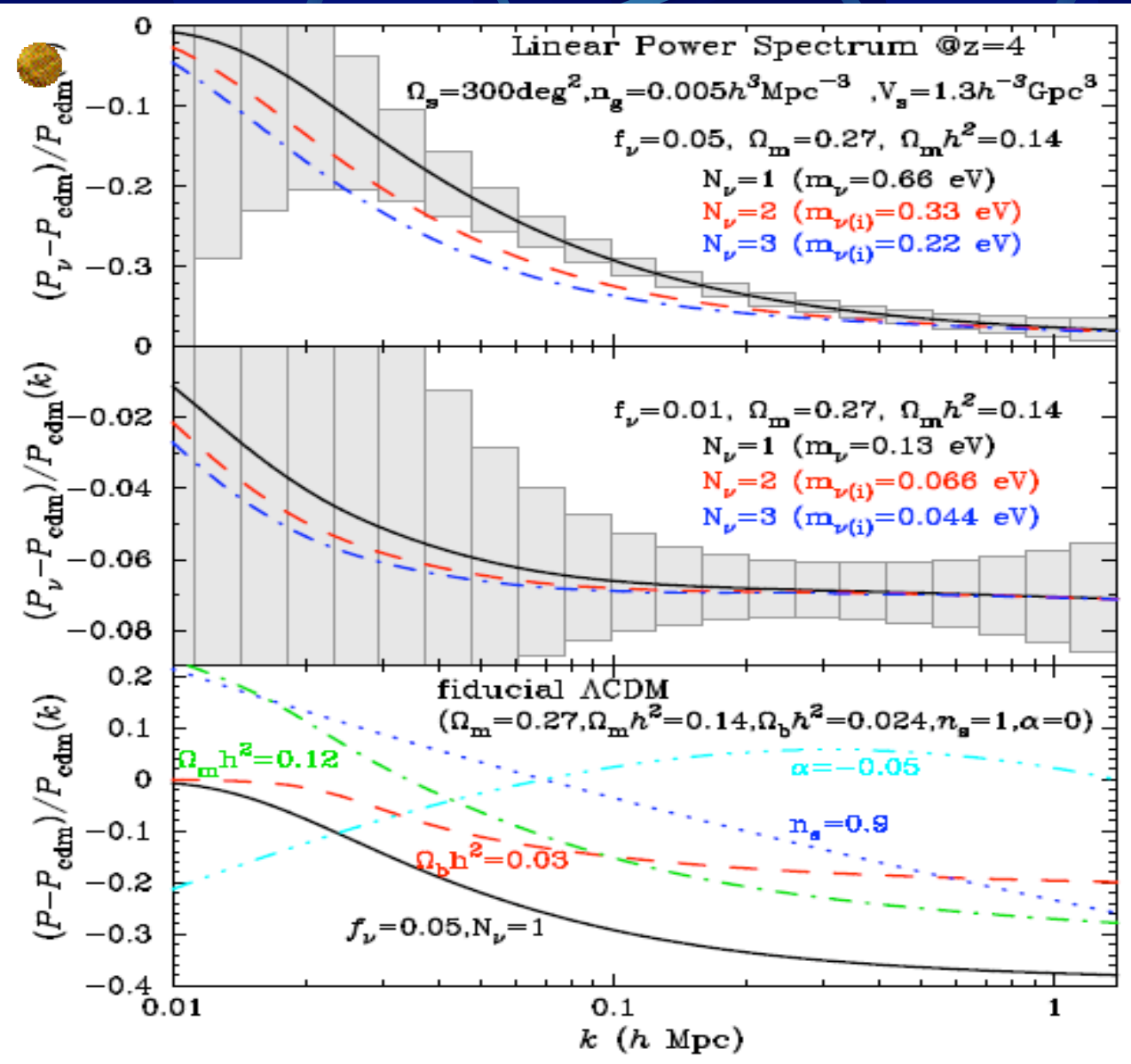


+’s mark the tilt and running predictions of single scalar-field models of Inflation that produce a flat (or nearly flat) Universe

$2\sigma$  constraint ellipse from WMAP (3-yr) + SDSS (LRG), after Tegmark *et al.* 2006

# Neutrino Mass

- Free-streaming of non-relativistic neutrinos suppress the amplitude of the matter power spectrum at small scales.
- The total suppression depends only on the total neutrino mass.
- The free-streaming scale depends on individual neutrinos mass.



# Parameter Forecast

*Takada, Komatsu & Futamase, PRD 73, 083520 (2006)*

Survey	$f_\nu (m_{\nu, \text{tot}} \text{ eV})$	$N_{\nu, \text{fid}}^{\text{nr}} = 1 \quad N_{\nu, \text{fid}}^{\text{nr}} = 2 \quad N_{\nu, \text{fid}}^{\text{nr}} = 3$			$n_s$	$\alpha_s$	$\Omega_m$	$\ln \delta_\zeta$	$\ln \Omega_m h^2$	$\ln \Omega_b h^2$
		$N_\nu^{\text{nr}}$	$N_\nu^{\text{nr}}$	$N_\nu^{\text{nr}}$						
Planck alone	–	–	–	–	0.0062	0.0067	0.035	0.013	0.028	0.011
G1	0.0045(0.059)	0.31	0.64	1.1	0.0038	0.0059	0.0072	0.0099	0.0089	0.0075
<b>HETDEX</b>	0.0033(0.043)	0.20	0.49	0.90	0.0037	0.0057	0.0069	0.0099	0.0086	0.0072
<b>CIP</b>	0.0019(0.025)	0.14	0.40	0.80	0.0030	0.0024	0.0041	0.0090	0.0055	0.0050
All (G1+G2+SG)	0.0018(0.024)	0.091	0.31	0.60	0.0026	0.0023	0.0030	0.0089	0.0043	0.0048

- CIP, in combination with the CMB data from Planck, will **determine the tilt and running to a few  $\times 10^{-3}$  level.**
- The running predicted by a very simple inflationary model (a massive scalar field with self-interaction) predicts the running of  $(0.8-1.2) \times 10^{-3}$ , which is not very far away from CIP's sensitivity.
  - More years of operation, or a larger FOV may allow us to measure the running from the simplest inflationary models.
- The limit on neutrino masses will be 20-40 times better than the current limit.

- We are 3/4 of the way through the theory of  $P(k)$  for high- $z$  galaxy surveys.
  - Non-linear matter evolution
  - Non-linear bias
  - Non-linear Kaiser effect
  - △ Finger of God effect
- “Almost ready” for interpreting the data from high- $z$  surveys (HETDEX, WFMOS & CIP)
- A better model for the Finger of God effect beyond an ansatz is required for extracting more cosmological information.